UNIVERSIDADE DE LISBOA

FACULDADE DE FARMÁCIA

Insight on the function of MyT1L in Ascl1 mediated neuronal reprogramming

Diogo Miguel Rosa Tomaz

DISSERTAÇÃO

MESTRADO EM CIÊNCIAS BIOFARMACÊUTICAS

Biologia do Desenvolvimento

2015

UNIVERSIDADE DE LISBOA

FACULDADE DE FARMÁCIA

Insight on the function of MyT1L in Ascl1 mediated neuronal reprogramming

Diogo Miguel Rosa Tomaz

Dissertação orientada pelo Doutor Diogo Castro

Orientador Interno: Professora Susana Solá

MESTRADO EM CIÊNCIAS BIOFARMACÊUTICAS

2015

The studies presented in this thesis were carried out at the Instituto Gulbenkian Ciência (IGC) at the Molecular Neurobiology Laboratory, Oeiras. The present study was supported by Fundação Calouste Gulbenkian.

FUNDAÇÃO CALOUSTE GULBENKIAN
Instituto Gulbenkian de Ciência

Index

Acknoledgements

I would like to thank to:

My supervisor Diogo Castro for sharing his knowledge; for addressing my doubts and questions; and for guiding my work in the right direction and helping me mature my scientific reasoning.

The molecular neurobiology laboratory current and former members Alexandre Raposo, Cátia Laranjeiro, Francisca Vasconcelos, Mário Soares, Pedro Rosmaninho, Vera Teixeira and our the wing technician Sónia Rosa for helping with the laboratory techniques, patiently explaining the answers to my questions and for smiling to my bad jokes.

All the IGC members that helped me throughout this year, especially to Joana Nabais, Tânia Ferreira, José Planells, Inês Almeida, Sandra Tavares for reagents, protocols and helpful discussions.

My co-supervisor for helping me in the writing of the dissertation and for always being available to my questions.

Aos meus amigos Afonso Bravo, Alicia Calvo-Villamañán, André Salvada e Daniel Eleutério pelos encontros esporádicos mas que sempre proporcionaram bons e divertidos momentos.

À Vânia Veiga por sempre poder contar contigo para me animares quer pelas tuas parvoíces, quer por pacientemente aturares as minhas.

À minha mãe, pai, irmão e sobrinha pelo carinho, amor e alegria ao qual posso sempre contar.

List of abbreviations

aN1	Activated Notch1
Ascl1	Achaete-scute homolog 1
bHLH	Basic helix-loop-helix
bp	Base-pair
BSA	Bovine serum albumin
CAG	Cytomegalovirus immediate enhancer/β-actin
CMV	Cytomegalovirus immediate early promoter
ChIP	Chromatin immunoprecipitation
DAPI	4’,6’-diamidino-2.phenylindol
DMEM	Dulbecco’s Modified Eagle Medium
DOX	Doxycycline
eGFP	Enhanced green fluorescent protein
FAIRE	Formaldehyde-assisted isolation of regulatory elements
FBS	Fetal bovine serum
GAPDH	Glyceraldehyde-3-phosphate dehydrogenase
HA	Hemagglutinin
HEK293T	Human embryonic kidney cells
Hes1	Hairy and enhancer of split-1
Hes5	Hairy and enhancer of split-5
iN	Induced neuronal cell
MEF	Mouse embryonic fibroblast
MyT1	Myelin transcription factor 1

MyT1L	Myelin transcription factor 1-like
NaDOC	Sodium deoxycholate
NICD	Notch intracellular domain
NS/PC	Neural stem/progenitor cells
ORF	Open reading frame
PBS	Phosphate-buffered saline
PEI	Polyethylenimine
qPCR	Real-time quantitative polymerase chain reaction
RBPJ	Recombination signal binding protein for immunoglobulin kappa J region
RGA	Reporter gene assay
RT-qPCR	Reverse transcriptase quantitative real-time PCR
rtTA	Reverse tetracycline-controlled transactivator
TF	Transcription factor
TNR	Transgenic Notch Reporter
WB	Western blot

Summary

Previous studies have accomplished direct lineage reprogramming of many cell types to different ones by using defined combinations of transcription factors. Vierbuchen et al. showed that the combined ectopic expression of Ascl1, Brn2 and MyT1L can efficiently reprogram mouse embryonic fibroblasts (MEFs) into induced neuronal (iN) cells. In another study, Ascl1 was characterized as the main driver of this process by its activity as a pioneer factor. Previous experiments with Ascl1 single-reprogramming showed that Ascl1 is capable of converting MEFs into iN cells, although the reprogrammed neurons show low levels of maturity. On the other hand, several reprogramming experiments associated MyT1L with a late function by promoting the maturation of iN cells, but not with the capacity to reprogram MEFs into iN cells like Ascl1. However, a mechanistic characterization of MyT1L still needed to be clarified.

MyT1L is a member of the MYT1 family, also including MyT1 and MyT3, all zinc-finger transcription factors. Recent work from our laboratory showed that MyT1, a paralog of MyT1L, acts as a repressor of Notch targets, in neural stem/progenitor cells. One of those identified Notch targets was Hes1. In neurogenesis, the Notch pathway induces the activation of the Notch downstream effector Hes1. Hes1 functions as a repressor of proneural genes, such as Ascl1, as well as their target genes. Similar to the neurogenesis context, it is tempting to speculate that in Ascl1-dependent reprogramming Hes1 may be functioning as a repressor of Ascl1 targets in MEFs.

The goal of this work is to investigate the role of MyT1L and the Notch signalling pathway in Ascl1-dependent reprogramming of MEFs into iN cells.

To evaluate Notch activity in MEFs, I compared the expression levels of two Notch targets, Hes1 and Hes5, between MEFs and neural stem cells. I show that Hes1 expression in MEFs is similar to Hes1 expression in neural stem cells. Hes5 expression is substantially lower in MEFs than in neural stem cells. This suggests low Notch activity in MEFs as previous studies identify the *Hes5* promoter as readout of Notch activation.

Chemical inhibition of Notch signalling did not alter the Hes1 expression in MEFs. I show that the proximal promoter region of *Hes1*, that mediates regulation by Notch and MyT1 in neural stem/progenitor cells, is accessible to transcription factor binding in MEFs. Additionally, I show that the Notch effector transcription factor RBPJ binds to the *Hes1* proximal promoter region. These results in conjunction with the high levels of Hes1 expression in MEFs suggest that the Notch pathway is not the main regulator of Hes1 expression in these cells.

Work from our laboratory showed that, in transcriptional assays, MyT1 represses the *Hes1* proximal promoter activity, after Notch activation. Here I show that Myt1L can counteract the Notch activation of the *Hes1* promoter in a transcriptional assay. The *Hes1* proximal promoter contains three consensus binding sites of the MYT1 family suggesting that MyT1L regulates the *Hes1* promoter by direct DNA-binding to this region. Using chromatin immunoprecipitation assay against a tagged version of Myt1L, I show that MyT1L directly binds to the *Hes1* promoter region two days after being ectopically expressed in MEFs.

Finally I started the optimization of the Ascl1-depedent reprogramming protocol in MEFs. I did observe reprogrammed iN cells after single or combined expression of Ascl1 or Ascl1/MyT1L, respectively. However, the percentage of iN cells to total number of cells in culture revealed low reprogramming efficiency. Additionally, iN cells observed show low levels of maturity in single or combined expression of Ascl1 or Ascl1/MyT1L. Nonetheless, this protocol still needs further improvement.

Overall, my findings indicate that MyT1L binds to DNA in MEFs at early stages of the Ascl1-dependent reprogramming protocol. The results suggest that MyT1L represses the expression of Hes1 in Ascl1-dependent reprogramming and this may lead to the activation of the Ascl1 targets that promote iN cell maturation.

Keywords

Ascl1; Neuronal Reprogramming; Notch signalling pathway; MyT1L; Hes1

Sumário

Vários estudos têm vindo a demonstrar que a reprogramação directa de uma linha celular somática para outros tipos celulares pode ser alcançada através da expressão ectópica de factores de transcrição. De facto, trabalho desenvolvido por Yamanaka e Takahashi (Takahashi and Yamanaka, 2006) demonstrou que a adição de quatro factores de transcrição é suficiente para reprogramar fibroblastos em células estaminais pluripotentes. Este estudo estabeleceu uma mudança de paradigma na forma como olhamos para o programa de transcrição e a plasticidade do genoma da célula. A reprogramação de um tipo celular a partir de células estaminais ou somáticas oferece um enorme potencial de aplicações na medicina regenerativa e na terapia de doenças.

A reprogramação de fibroblastos em células neuronais foi alcançada através da adição de três factores de transcrição, Brn2, Ascl1 e MyT1L (BAM) (Vierbuchen et al., 2010), em que o Ascl1 é o factor de transcrição principal, uma vez que, sozinho, é capaz de converter os fibroblastos em neurónios, apesar de apresentarem baixa complexidade morfológica e capacidade funcional (Chanda et al., 2014). Curiosamente, Ascl1 funciona como um factor pioneiro, sendo capaz de se associar às regiões genómicas, independentemente de se encontrarem em locais de cromatina acessível (Raposo et al., 2015; Wapinski et al., 2013).

O Ascl1 é um factor de transcrição proneural que actua como um regulador da diferenciação neuronal no cérebro de mamíferos (Bertrand et al., 2002; Wilkinson et al., 2013). No processo de neurogénese, Ascl1 actua principalmente como um activador de transcrição sobre uma grande variedade de genes que controlam vários passos da neurogénese, como a proliferação das células estaminais neurais/progenitoras, migração celular e crescimento das neurites (Borromeo et al., 2014; Castro et al., 2011, 2006). Recentemente, Ascl1 foi identificado como um factor de transcrição capaz de modificar a cromatina dos seus genes alvos, durante a neurogénese, promovendo a acessibilidade da cromatina para Ascl1 (Raposo et al., 2015).

Durante a neurogénese, o Ascl1 é regulado pela via de sinalização Notch. No desenvolvimento do sistema nervoso, a via de sinalização Notch é responsável pela manutenção da população de células estaminais neuronais/progenitoras, através da inibição da diferenciação neuronal. A proteína Notch activa a expressão de genes repressores da neurogénese, dos quais se incluem os genes *Hes1* e *Hes5*. Os genes *Hes1/5* actuam como repressores da transcrição, sendo um dos seus alvos *Asc1*. Adicionalmente, resultados anteriores do nosso laboratório demonstraram que Hes1 inibe a expressão dos genes alvos de Ascl1.

Recentemente, estudos realizados no nosso laboratório revelaram que um alvo de Ascl1 durante a neurogénese, o factor MyT1, tem um papel importante em bloquear a expressão de genes alvo de Notch, em particular o *Hes1*. MyT1 é um factor de transcrição da família MYT1, que é composta por outros 2 factores de transcrição: MyT1L e MyT3. Os membros desta família são altamente homólogos, particularmente nos domínios proteicos *zinc-fingers,* responsáveis pela ligação ao ADN (Bellefroid et al., 1996; Kim et al., 1997). Todos os membros da família MYT1 são expressos no desenvolvimento do sistema nervoso central. Em particular, MyT1L é expresso exclusivamente em neurónios e é detectado tanto na neurogénese como na fase adulta do organismo (Matsushita et al., 2014). Na reprogramação neuronal, o MyT1L tem sido utilizado em vários protocolos para promover um aumento da complexidade morfológica e das propriedades electrofisiológicas das células neuronais (Ambasudhan et al., 2011; Pang et al., 2011; Vierbuchen et al., 2010; Yoo et al., 2011). Considerando os resultados do nosso laboratório em que se demonstrou que MyT1 é um repressor da expressão de Hes1, colocámos a hipótese de que MyT1L pudesse também actuar na reprogramação de células neuronais como um repressor da expressão de Hes1.

O trabalho desta dissertação teve como objectivo investigar o papel do MyT1L e da via de sinalização Notch na reprogramação de fibroblastos em células neuronais promovida por Ascl1.

Em primeiro lugar analisei a actividade da via de sinalização Notch nos fibroblastos através da análise de expressão de dois genes alvos de Notch, *Hes1* e *Hes5*. A expressão destes genes foi comparada entre fibroblastos e células NS-5, uma linha de células estaminais neurais com elevada actividade da via Notch. Os resultados demonstraram que o nível de expressão de *Hes1* em fibroblastos e em células NS-5 são semelhantes. No entanto, após inibição química da actividade de Notch não observei nenhuma alteração na expressão de *Hes1*, o que sugere que a via sinalização Notch não é a principal reguladora de *Hes1* nos fibroblastos. Contrariamente a *Hes1*, a expressão de *Hes5* é consideravelmente inferior nos fibroblastos em relação às células NS-5. Por outro lado, a inibição química da actividade de Notch levou a uma diminuição da actividade da expressão de *Hes5*, indicando que *Hes5* é regulado por Notch em fibroblastos.

Em segundo lugar, investiguei qual o possível papel de MyT1L na regulação da expressão de Hes1 em fibroblastos. Analisei que a região promotora de *Hes1*, onde anteriormente o nosso laboratório demonstrou haver associação de MyT1 em células neurais/progenitoras estaminais, se encontra com cromatina acessível à associação de factores de trancrição, em fibroblastos. Também analisei a actividade de MyT1L nessa região promotora de *Hes1* através de um ensaio de transcrição com a co-expressão de MyT1L e receptor Notch1 activado. Esta análise revelou que o MyT1L é um repressor do promotor de *Hes1,* dependente da activação

pela via Notch. Esta região promotora de *Hes1* contém três sítios de ligação ao ADN comum à família MYT1. De facto, os resultados da imunoprecipitação da cromatina extraída de fibroblastos revelaram uma associação do MyT1L ectopicamente expresso na região promotora de *Hes1*.

Hes1 é um factor repressor da expressão de Ascl1 e dos seus genes alvos. De facto, é possível que, no contexto da reprogramação promovida por Ascl1, os níveis de Hes1 endógeno possam estar a reprimir a expressão dos genes alvos de Ascl1. Esta repressão de Hes1 pode explicar o baixo nível de diferenciação das células neuronais observado na reprogramação com apenas sobre-expressão de Ascl1. De facto, MyT1L foi descrito como tendo um papel importante no desenvolvimento de características de neurónios morfologicamente complexos. Assim é possível que, o MyT1L promova indirectamente a expressão dos genes alvos de Ascl1, através da inibição da expressão de Hes1. Deste modo, o protocolo de reprogramação de fibroblastos em células neuronais mediado por Ascl1 foi optimizado, com o objectivo de investigar a interacção de MyT1L e Hes1, no contexto desta reprogramação. Infelizmente, o protocolo não foi estabelecido com sucesso, devido, a uma elevada taxa de morte célular. Apesar da elevada morte celular, consegui obter células neuronais, a partir de fibroblastos, com apenas a sobre-expressão de Ascl1 em co-expressão com MyT1L. As células neuronais obtidas com estas duas condições apresentavam baixos níveis de complexidade morfológica.

Em conclusão, demonstrei que MyT1L encontra-se associado à região promotora de *Hes1* quando expresso de modo ectópico em fibroblastos e que Myt1L actua como um repressor da actividade da região promotora de *Hes1* promovida pela activação da via de sinalização Notch. A junção destes dois resultados sugere que a inibição da expressão de Hes1 se reflicta nos fibroblastos após sobre-expressão de Myt1L. A função de MyT1L pode incluir a repressão da expressão de Hes1, promovendo a activação de genes alvos de Ascl1 responsáveis pela maturação neuronal. Experiências futuras que demonstrem uma diminuição da expressão de Hes1 após a sobre-expressão de MyT1L em fibroblastos devem ser consideradas. Adicionalmente, futuras experiências devem também focar-se na descoberta de outros genes alvo de MyT1L em fibroblastos que possam ter um papel importante na reprogramação promovida por Ascl1 de fibroblastos em neurónios.

Palavras-chave

Ascl1; Reprogramação neuronal; Via sinalização Notch; MyT1L; Hes1

Introduction

During mammalian development, intrinsic transcriptional programs driven by transcription factors (TFs) are combined with cell extrinsic cues to establish cell identity. Interestingly, some TFs are able to active their transcriptional program when ectopically expressed in non-native cell types. Namely, the basic helix-loop-helix (bHLH) TF MyoD induced muscle-specific properties in fibroblasts (Davis et al., 1987). More recently, a study by Yamanaka and Takahashi (Takahashi and Yamanaka, 2006) demonstrates that the overexpression of four TFs (Oct4, c-Myc, Sox2 and Klf4) is sufficient to reprogram mouse embryonic fibroblasts (MEFs) into induced pluripotent stem cells (iPSCs). This study established a paradigm shift in how we look at transcriptional programs and genome plasticity. Since then, a variety of other studies used the expression of defined combinations of transcription factors to reprogram cells into pluripotency or different somatic lineages: Stadfield *et al*. demonstrated that pancreatic β cells can be reprogrammed to iPSCs by overexpressing the same four TFs used by Yamanaka and colleagues; also, fibroblasts have been successfully reprogrammed to a variety of other somatic lineages, like cardiomyocytes, hepatocytes and neurons, utilizing TFs specific to each lineage (Huang et al., 2011; Ieda et al., 2010; Vierbuchen et al., 2010). Lineage conversion from embryonic stem cells (ESCs) and iPSCs or already differentiated somatic cells into other cell types, like neuronal cells, attracts vast interest due to its potential application in regenerative medicine and in the therapy of developmental diseases (Blanpain et al., 2012; Marchetto and Gage, 2012).

Of specific interest to this dissertation is the first reported study in which MEFs were directly reprogrammed into induced neuronal (iN) cells by simultaneous overexpression of three TFs, Brn2, Ascl1 and MyT1L (BAM) (Vierbuchen et al., 2010). Other studies followed on this reprogramming protocol, albeit with few modifications: conversion of adult human fibroblasts to iN cells was achieved by adding NeuroD to the initial BAM set; dopaminergic neurons can be induced by expressing the BAM set of factors plus Lmx1a and FoxA2, two regulators in dopamine neuron generation (Pang et al., 2011; Pfisterer et al., 2011). More recently, Ascl1 was found to be sufficient to reprogram fibroblasts into iN cells, although, these iN cells appear to be more immature than the iN reprogrammed with the full set of BAM factors (Chanda et al., 2014). Recent study at the mechanism of iN cells reprogramming by BAM set of factors revealed Ascl1 as the main factor that drives the reprogramming process. Ascl1 has the ability to function as an “on-target” pioneer factor in MEFs. This means Ascl1 binds directly to nucleosomal chromatin and to its *bona fide* targets in neural progenitors (Raposo et al., 2015; Wapinski et al., 2013).

Ascl1 is a basic Helix-loop-Helix (bHLH) proneural transcription factor that acts as a main regulator of neurogenesis in the mammalian brain, alongside other bHLH proneural factors expressed in neural stem/progenitor cells (NS/PCs) (Bertrand et al., 2002; Wilkinson et al., 2013). Proneural factors are both required and sufficient to induce a full program of neuronal differentiation. Accordingly, gain-of- and loss-of-function analysis of *Ascl1* show, respectively, capacity to induce full neuronal differentiation program and neural developmental defects associated with reduced neurogenesis (Casarosa et al., 1999; Geoffroy et al., 2009; Raposo et al., 2015). The use of genomic approaches has started to elucidate the mechanisms behind Ascl1 regulation of neurogenesis. Ascl1 functions as a transcriptional activator (Borromeo et al., 2014; Castro et al., 2006; Raposo et al., 2015) over a large number of effector genes that control various steps of neurogenesis, such as neuronal fate specification, progenitor proliferation, cell migration and neurite outgrowth (Castro et al., 2011). Furthermore, recent work revealed that Ascl1 also function as a pioneer factor in its native context, binding closed chromatin in some of its targets and promoting changes in the chromatin accessibility at its target sites during neurogenesis (Raposo et al., 2015).

During neurogenesis, Ascl1 is simultaneously regulated and is regulated by the Notch signalling pathway. Notch signalling is an evolutionary conserved pathway present in many tissues with a wide variety of functions (Andersson et al., 2011). In the developing nervous system it is responsible for the process of lateral inhibition, whereby a differentiating neuronal progenitor cell transiently inhibits differentiation of surrounding neural stem/progenitors cells from undergoing the same fate (Louvi and Artavanis-Tsakonas, 2006). Ascl1 induces Notch ligands, such as Delta1, at the transcriptional level. Delta1 binds to the Notch receptor at the cell surface triggering intracellular transmembrane proteases to cleave and release the Notch Intracellular Domain (NICD). NICD then is translocated to the nucleus where it binds to the downstream effector RBPJ. In the absence of Notch activity, RPBJ functions as a repressor at promoters of target genes (Castel et al., 2013). Upon Notch activation, RBPJ/ NICD form a complex with coactivators that will activate Notch target genes. Amongst these are Hes1 and Hes5, two bHLH proteins that function as transcriptional repressors. Hes1/5 can repress proneural factors such as Ascl1 which prevents neuronal differentiation and contributes to the maintenance of a pool of neural stem/progenitor cells (Figure 1A) (Hojo et al., 2000; Kageyama et al., 2005; Wu et al., 2003). Moreover, unpublished work from our laboratory shows that Hes1 additionally represses Ascl1 target genes. Recent studies showed that Notch direct and indirect targets, like *Hes1* and *Ascl1*, respectively, are expressed in an oscillatory manner (Imayoshi et al., 2013). This results from Hes1 functioning as an intrinsic oscillator, due to its ability to repress its own promoter, associated with its short-lived transcript and protein

(Hirata et al., 2002). At the same time, Ascl1 oscillates in an out-of-phase manner to Hes1 oscillation. These two modes of Ascl1 expression, oscillatory or sustained, are associated with distinct activities. When expressed in an oscillating mode, Ascl1 promotes cell proliferation. When Ascl1 is expressed at constant levels the NS/PCs undergo neuronal differentiation (Figure 1B) (Shimojo et al., 2011). What regulates the switch from an oscillatory to sustained mode of these TFs expression remains an important question in the field.

Recent work in our laboratory showed that regulation by Ascl1 of the expression of the zinc-finger factor MyT1 may play an important role in this process. MyT1 is a transcriptional repressor that regulates a large number of canonical Notch target genes. Importantly, MyT1 counteracts Notch mediated Hes1 activation (Figure 2A), by a mechanism that requires direct DNA binding to three consensus sites at the Hes1 proximal promoter region that partially overlap with RBPJ –binding sites (Figure 2B).

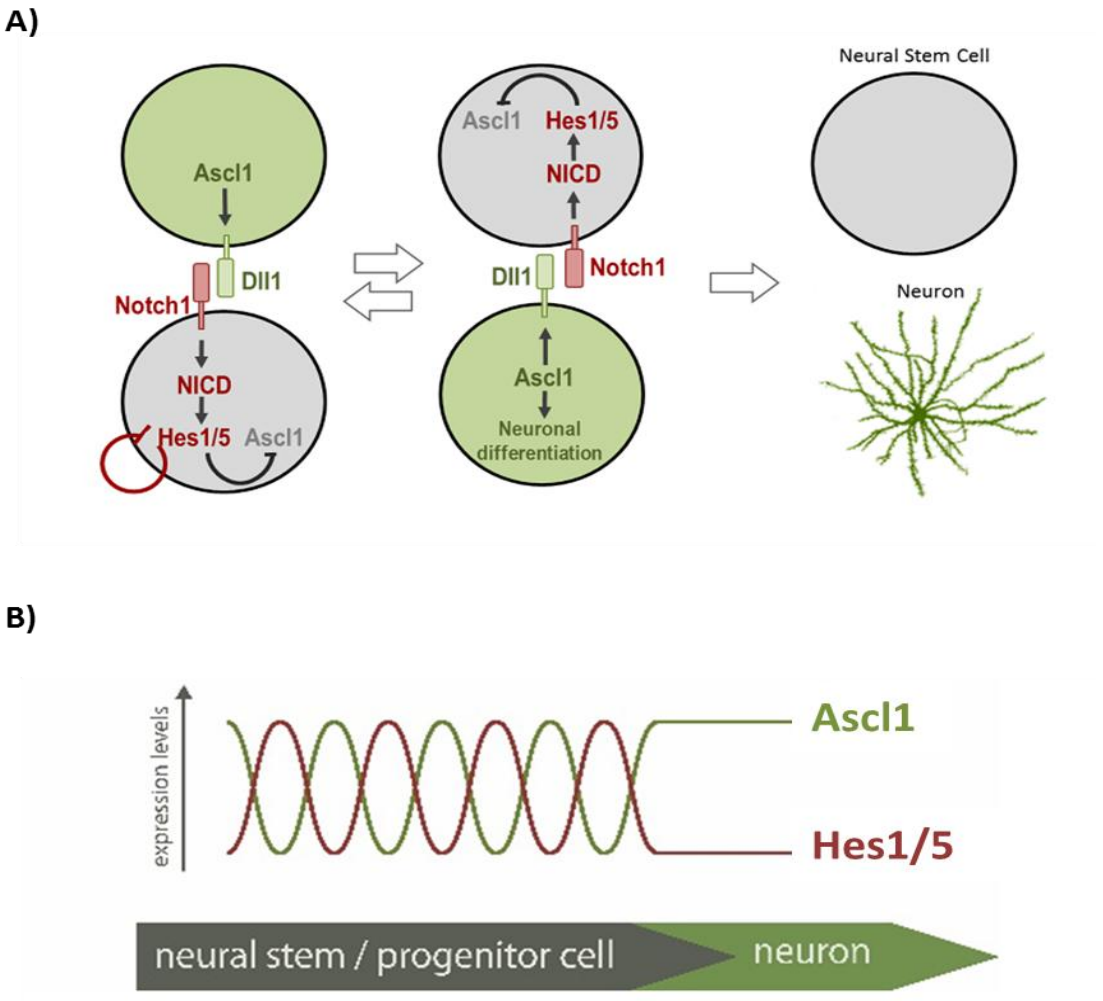

Figure 1 – Interplay between proneural factor Ascl1 and proneural repressors Hes1/5 at the onset of differentiation. **(A)** Notch signalling is activated through cell-cell interactions between the transmembrane proteins Delta-like1 (Dll1) and Notch1 receptor, expressed in neighbouring cells. In

differentiating NS/PCs Ascl1 (as well as other proneural factors) induces the expression of Dll1, which activates Notch signalling in the Notch1 receptor-expressing cell. Upon activation, the Notch intracellular domain (NICD) is cleaved and translocated into the nucleus where it will form an activator complex with RPBJ and induce the expression of downstream genes, such as Hes1/5. Hes1/5 repress the expression of Ascl1, thereby inhibiting neuronal differentiation, while the neighbouring cell with Ascl1 expression is driven to neuronal differentiation. **(B)** *Hes1/5* genes are intrinsic oscillators. The opposing interaction between Hes1/5 and Ascl1 proteins results in oscillation of these TFs in an out-of-phase pattern. At the onset of neurogenesis, Hes1 expression becomes permanently downregulated and, consequently, Ascl1 upregulation is sustained. Figures adapted from (Kageyama et al., 2008) and (Vasconcelos and Castro, 2014), respectively.

MyT1 belongs to a family comprised of 3 members: *MyT1* (NZF2), *MyT1L* (NZF1) and *MyT3* (NZF3 or st18) that encode structurally related zinc-finger (ZF) transcription factors. Members of this family are highly homologous, particularly within the DNA-binding ZF domains (Figure 3) (Bellefroid et al., 1996; Kim et al., 1997). All MYT1 family members are expressed throughout the mouse developing central nervous system (CNS). Specifically MyT1L is exclusively expressed in neurons, throughout neurogenesis and adulthood, and most prominently expressed in post-mitotic cells (Matsushita et al., 2014, 2002). Mouse genetics has failed so far to identify the function of MYT1 family members during development. No significant defects have been reported in the *MyT1* null embryo, which may be due to genetic redundancy resulting from the concomitant upregulation of *MyT1L* and *MyT3* (Wang et al., 2007). In reprogramming, MyT1L overexpression in a variety of neuronal reprogramming protocols has been associated with an enhancement of the morphological complexity and electrophysiological properties of the induced neurons (Ambasudhan et al., 2011; Pang et al., 2011; Vierbuchen et al., 2010; Yoo et al., 2011). Various lines of evidence from work conducted in our laboratory, including transcriptional assays using promoter-reporter gene constructs, implicate MyT1 in counteracting the activation of Notch-dependent activation of *Hes1*. Given that Hes1 has been reportedly expressed in MEFs (Yoshiura et al., 2007), it is tempting to speculate that MyT1L may function in Ascl1-dependent reprogramming by repressing *Hes1* expression.

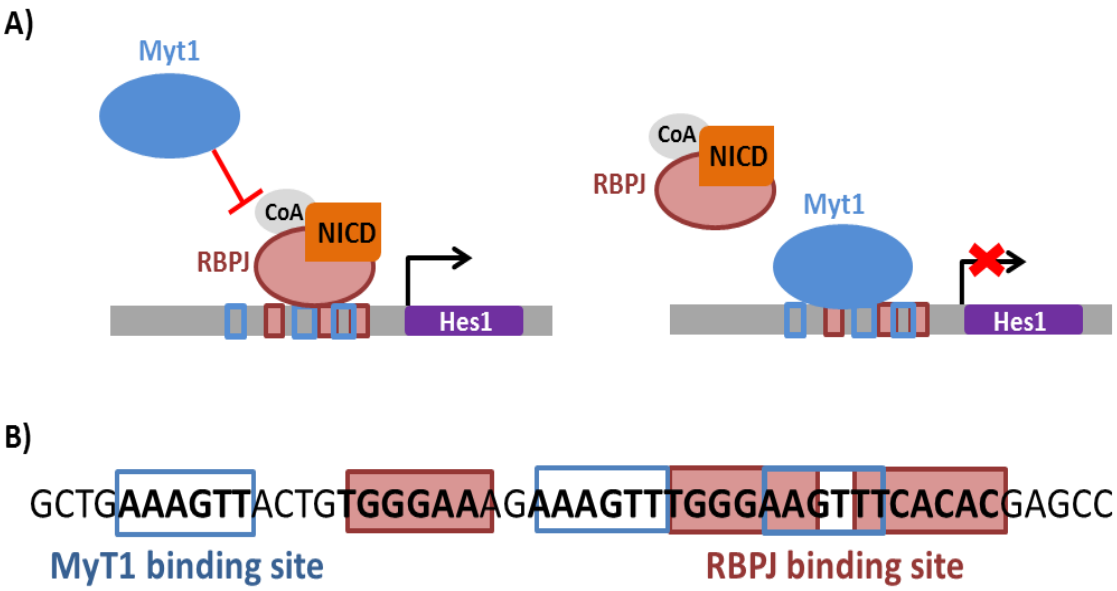

Figure 2 – MyT1 regulation of the *Hes1* proximal promoter by direct DNA-binding. **(A)** MyT1 counteracts Notch activation of Hes1 promoter by direct DNA binding and competition with NICD/RBPJ activator complex for DNA binding. **(B)** Hes1 proximal promoter region contains three MyT1 binding sites interspersed and partially overlapping with three RBPJ binding sites. Figure adapted from results obtained from our laboratory (Vasconcelos, personal communication).

The goal of this work is to investigate the role of MyT1L and the Notch signalling pathway in Ascl1-dependent reprogramming of MEFs into iN cells. I first determined whether Notch signalling is active in MEFs namely its function in regulating Hes1 expression. Secondly, I focused on the TF MyT1L and its possible role in regulating Hes1 expression when ectopically expressed in MEFs. Thirdly, I attempted to establish the Ascl1-dependent reprogramming protocol, with the aim of investigating the interaction of MyT1L and Hes1 in this context.

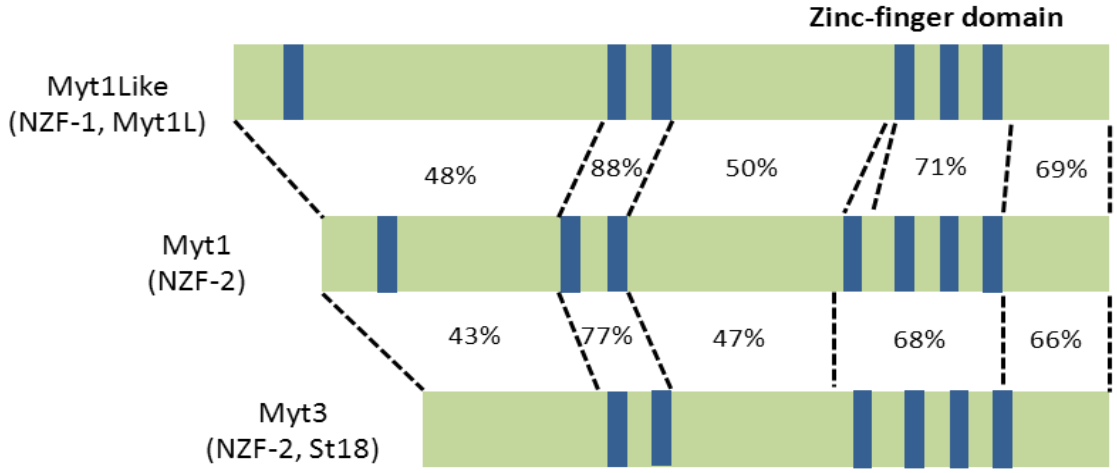

Figure 3 – MYT1 family members. Scheme portrays the structural comparison between members of the MYT1 family of transcription factors: MyT1L (1188 amino acis), MyT1 (1127 amino acis) and MyT3 (1045 amino acids). The blue boxes indicate C2HC-type zinc finger domains. Percentages conservation of

various protein domains (set apart by dashed lines) between MyT1L and other members are shown. Figure refers to proteins encoded by mouse genes. Figure adapted from (Matsushita et al., 2014).

Materials and methods

1. Animals

All experiments with NMRI (Charles River) and Transgenic Notch Reporter mice (Jackson Laboratories) were carried out upon approval and following the guidelines of the ethics committee of Instituto Gulbenkian de Ciência.

2. Molecular Biology

2.1. Expression vectors

The expression vectors are listed on Table 1.

Table 1 - Expression vectors

Vector	Reference
pCAG-MyT1L	(Kameyama et al., 2011)
pCAG-MyT1L-HA	Generated during this work
pCAG- MyT1-IRES-GFP	(Vasconcelos et al. Unpublished)
pCAG-acNotch1	Gift from Ryoichiro Kageyama
p3xFlag-CMV7-NICD1	(Ong et al., 2006)(Addgene #20183)
pCMV-βgal	

2.2. Luciferase reporter vectors

The expression vectors are listed on Table 2.

Table 2 – Luciferase reporter vectors

Vector	Genomic coordinates	Reference
Hes1:Luc	chr16:30064977-30065489	(Nishimura et al., 1998) (Addgene #41723)

2.3. Lentiviral vectors

The expression vectors are listed on Table 3.

2.4. Transformation into chemically competent *E.coli*

100µL of chemically competent *E.coli* DH5α were incubated with approximately 500ng of vector DNA for 15min on ice. After a 60sec heat shock at 37ºC the bacteria were chilled on ice for at least 2min, ~250µL LB was added. The bacteria were incubated for ~1h at 37ºC on a shaker incubator, subsequently plated on LB_{Amp} plates and placed overnight at 37ºC.

Table 3 – Lentiviral vectors

Vector	Reference
TetOn-FUW-V5-Ascl1	Gift from Marius Wernig
TetON-FUW-MyT1L-HA	Generated during this work
TetON-FUW-MyT1L	(Vierbuchen et al., 2010)(Addgene #27152)
TetON-FUW-eGFP	(Vierbuchen et al., 2010)(Addgene #30130)
TetON-FUW empty	Generated during this work
FUW-M2rtTA	(Hockemeyer et al., 2008) (Addgene #20342)

2.5. DNA purification

Plasmids were isolated from *E.coli* DH5α using Qiagen's Mini, Midi or Maxi-Prep Kits. PCR-Products were purified with the Qiagen's PCR Purification Kit, DNA bands from agarose gels were purified with the Qiagen's Gel Extraction Kit. All steps were performed as recommended by the supplier. For phenol-chloroform extraction, one volume of phenol:chloroform:isoamyl alcohol 25:24:1 (Sigma-Aldrich) was added. The mixture was vortexed shortly and centrifuged for 5min at maximum speed in a tabletop microcentrifuge. Upper phase was recovered and 1/10 volume of 3M sodium acetate and 0.7 volumes of 100% ethanol (RNase free) were added to precipitate DNA. Sample was incubated for 30-60min at RT and centrifuged (10min at RT, 13000rpm). Supernatant was discarded and the pellet was washed with 70% ethanol. After air drying, the pellet was re-suspended in an appropriate volume of RNAse and DNase-free water (Sigma-Aldrich).

2.6. DNA restriction digestion

For sub-cloning digestions were performed in 50µL total volume with 1-2µg DNA and ~ 2units enzyme overnight at 37ºC.

2.7. Vector dephosphorylation

Dephosphorylation procedure was performed with purified pre-digested vector and 2µL of Antarctic phosphatase (New England Biolabs) to a total volume of 20µL for 15min at 37ºC. Heat inactivation of the enzyme was carried out by incubating the mixture for 5min at 65ºC.

2.8. Ligation

Ligations were performed with a 10:1 or 3:1 molar ratio insert/vector, for blunt end or sticky end ligations, respectively, using the DNA and Takara Long ligation kit (Takara Bio) according to manufacturers' instructions. Samples were incubated at 16ºC overnight and transformed the next day. Colonies were selected and inoculated in LB medium with Ampicillin

at 37ºC overnight. To confirm the correct insertion of the insert into the vector, digestion was performed at 37ºC for 1.5h and the resulting products were analyzed on a 1% agarose gel.

2.8.1 .pCAG-Myt1L-HA

To generate MyT1L tagged C-terminally with influenza hemagglutinin tag (HA tag), an HA tag oligonucleotide was inserted into the pCAG-MyT1L by amplifying a fragment of the cDNA using an overhang on the Reverse Primer containing the HA tag, STOP codon, one *EcoR*I site and one *Bgl*II site (Table 4). The amplified fragment and the pCAG-MyT1L were digested for *Sac*I and *Bgl*II, and then ligated overnight. Bacteria were transformed and positive colonies were screened by digesting the purified DNA with *Hind*III and *EcoR*I and by subsequent analysis of digestion pattern in agarose gel. Positive colonies were sequenced to confirm the lack of mutations. The pCAG-MyT1L-HA has less 9 nucleotides in the *MyT1L* cDNA than the pCAG-MyT1L resulting from the strategy employed to remove one *EcoR*I site present in the *MyT1L* cDNA, near the C-terminal. This was necessary to facilitate further sub-cloning strategies.

Table 4 – Primers for Myt1L-HA sub-cloning

Primers	Forward Primer	Reverse Primer
MyT1L-HA	GCGGACAAAAAGCATTCGAAGTATG	GATGATAGATCTGAATTCTCAAGCGTAATCTGGTACG TCGTATGGGTATCCTCTCACAGCCTGCTTTATATTTTC

2.8.2. TetON-FUW Myt1L-HA

MyT1L-HA was excised from pCAG-MyT1L-HA vector using *EcoR*I restriction enzyme and purified via agarose gel.

The TetON-FUW V5-Ascl1 was digested with *EcoR*I and the TetON-FUW backbone was purified via agarose gel.

TetON-FUW backbone and MyT1L-HA fragment were ligated overnight. Bacteria were transformed and positive colonies were screened by digesting the purified DNA with *Stu*I and by subsequent analysis of the digestion pattern in agarose gel. Positive colonies were sequenced to confirm the lack of mutations.

2.8.3. TetON-FUW empty

V5-Ascl1 was excised from TetON-FUW V5-Ascl1 with *EcoR*I. The TetON-FUW backbone was purified via agarose gel. TetON-FUW backbone was re-ligated overnight. Bacteria were transformed and positive colonies were screened by digesting the purified DNA with *EcoR*I and

by subsequent analysis of the digestion pattern in agarose gel. Positive colonies were sequenced to confirm the lack of mutations.

3. Cell culture

3.1. Cell line generation and maintenance

Mouse embryonic fibroblasts (MEFs) were isolated from E12.5 embryos under a dissection microscope (Nikon). The head, vertebral column (containing the spinal cord), dorsal root ganglia and all internal organs were removed and discarded to ensure the removal of all cells with neurogenic potential from the cultures. The remaining tissue was manually dissociated and incubated 0.25% trypsin (Gibco) for 10-15 min to create a single cell suspension. Cells from each embryo were plated onto a T150 flask with MEF media (Dulbecco's Modified Eagle Medium (DMEM)/ High glucose containing 10% fetal bovine serum (FBS) (both from BioWest), 2mM L-Glutamine and 100U/mL Penicillin/Streptomycin (both from Gibco)). Cells were grown at 37 °C until confluent and then split once before being frozen. After thawing cells were cultured on T-flasks and allowed to become confluent before being split onto well-plates (Corning) for infections using 0.25% trypsin.

Notch signalling inhibition of MEFs was performed by adding the γ-secretase inhibitor LY-411575 (Sigma-Aldrich) (Lanz et al., 2004) to the culture to a final concentration of 10nM, for 4 hours.

3.2. NS-5, P19 and HEK293T cells culture

NS-5 cells (Conti et al., 2005) were cultured in mouse Neurocult NSC basal medium supplemented with Neurocult NSC proliferation supplement (both from Stem Cell Technologies), 100U/mL Penicillin/Streptomycin (Gibco), 10ng/mL EGF (Peprotech), 10ng/mL bFGF (Peprotech) and 1µg/mL Laminin (Sigma-Aldrich) in T-flasks or well-plates.

P19 embryonic carcinoma cells and human embryonic kidney cells (HEK293T) were maintained in DMEM / High glucose supplemented with 10% FBS, 2mM L-Glutamine and 100U/mL Penicillin/Streptomycin in T-flasks or well-plates.

3.3. Transfection of P19 and HEK23T cells

On the previous day, P19 and HEK293T were plated to obtain a75% confluency on the day of the transfection. Transfection was carried out with linear polyethylenimine (PEI) (Sigma-Aldrich) in the proportion of DNA:PEI (w/w) of 1:2.5 for P19 cells and 1:3 for HEK293T cells. Total amount of DNA/cm^2: 500 ng. Medium was replaced with fresh medium 4-6h after transfection.

3.4. Lentivirus production and infection of MEF cells

Replication-incompetent lentiviruses were produced by transient transfection of HEK293T cells with TetON-FUW vectors or with FUW-M2rtTA cotransfected with the viral 2nd generation packaging vector psPAX2 and the viral envelope vector pVSV-G. Medium was replaced with fresh medium 6-8h post transfection. Two days after medium replacement, lentiviral particles were concentrated from supernatant by ultracentrifugation at 90000g for 4h at 4 °C and re-suspended in 0.1% bovine serum albumin (BSA, Promega) in Phosphate-buffered saline (PBS). Viral titter was verified after each production by infecting MEFs followed by immunofluorescence two days after induction. The number of infected cells was determined by visual counting immune-positive cells over all DAPI-positive nuclei.

MEFs infection was performed with V5-Ascl1, MyT1L-HA or Empty lentivirus, eGFP (enhanced green fluorescent protein) lentivirus, and reverse tetracycline transactivator (rtTA) lentivirus in a ratio of 1:1:1. Exception was the V5-Ascl1 and Myt1L-HA lentivirus co-infection were the eGFP lentivirus was not added to the lentiviral mix.

4. Dual luciferase reporter gene assay

P19 cells were seeded into 48-well plates at a density of 70 000 cells/cm2. Cells were transiently cotransfected with expression plasmids, firefly luciferase reporter plasmid and pCMV-β-galactosidase plasmid as an internal control. 24-36h after transfection, cells were lysed with RGA lysis buffer (Potassium phosphate 100µM pH7.8, 1uM EDTA, 10% glycerol, 1% Triton X-100, 1µM DTT (All from Sigma-Aldrich) in MilliQ water). Cell lysates were assayed for luciferase and β-galactosidase activities. Fold induction represents the values of (luciferase activity/β-galactosidase activity) for each condition normalized to control condition. Data are presented as mean ± SD of quadruplicate assays.

5. Protein lysates preparation

HEK293T cells were transiently transfected with expression constructs using PEI as described above. 24h post transfection cells were washed once with PBS and harvested by scraping in ice-cold lysis buffer (50mM Tris HCl pH 8.0, 150mM NaCl, 10% Glycerol, 0.1% NP-40 (all from Sigma-Aldrich), proteinase inhibitors (Roche) and protein quantification was carried out using Bradford method.

6. Western Blot (WB)

Crude cell lysates samples were diluted in 2x Laemmli buffer (Sigma-Aldrich) and denatured for 5min at 95ºC. Samples were separated in 10-12% SDS-PAGE gels and transferred to

nitrocellulose membranes (GE Healthcare) using standard procedures. Blots were probed with the primary and HRP-conjugated secondary antibodies listed on Table 5.1 and 5.2.

Table 5.1 – Primary antibodies used in Western blot

Antigen (species)	Working dilution in WB	Catalog number	Company/Reference
HA-tag (rabbit)	1:4000	ab9110	Abcam
α-tubulin	1:10000	T6074	Sigma-Aldrich

Table 5.2 – Secondary antibodies used in Western blot

Antigen (species)	Working dilution in WB	Company/Source
Goat Anti-Rabitt IgG (H+L) Poly-HRP	1:5000	Jackson ImmunoResearch
Donkey Anti-Mouse IgG (H+L) Poly-HRP	1:5000	Jackson ImmunoResearch

7. MEFs reprogramming into iN cells

MEFs were plated in 24-well plates with non-coated coverslips. Infection was performed, 24h after plating, in MEF media containing 8µg/mL polybrene (Sigma-Aldrich). After 16-20h in media containing lentivirus, the cells were switched into fresh MEF media containing 2µg/mL doxycycline (DOX, Sigma-Aldrich) to activate expression of the transduced genes. After 48h media was replaced by N3 media (DMEM/F12 w/ Glutamax (Gibco) containing 25µg/mL, 50µg/mL transferrin, 30nM sodium selenite, 20nM progesterone, 100nM putrescine dihydrochloride (All from Sigma-Aldrich) and 100U/mL Penicillin/Streptomycin) or N2B27 media (DMEM/F12 w/ Glutamax containing 25µg/mL insulin, 1x N2 supplement, 1x B27 supplement and 100U/mL Penicillin/Streptomycin). Media was changed every 2-3 days for the duration of the culture period.

8. Immunofluorescence

MEFs were grown on glass coverslips and washed with PBS before fixation with 4% formaldehyde for 10min and quenching with 0.1M Tris pH 7.4 for additional 10min. Cells were then incubated in 0.3% Triton X-100 in PBS for 10min at room temperature. Cells were blocked in a solution of PBS containing 0.1% Tween20 (Sigma-Aldrich) and 10% Normal Goat Serum (Cell Signalling Technology) in PBS for 60min (NGS, Gibco) at room temperature. Primary antibody and secondary antibodies were diluted in the blocking solution. Primary antibody was incubated at 4 °C overnight and secondary antibodies were incubated at room temperature for 45min. Cells were washed at room temperature three times for 5min with 0.05% Tween20 in

PBS between primary and secondary staining. Cell nuclei were stained with DAPI (4',6-diamidino-2-phenylindole; Sigma-Aldrich) (1:10000) before mounting in Aqua Poly/Mount (Polysciences). Cells were stained with the primary and secondary antibodies listed on table 6.1 and 6.2.

Table 6.1 – Primary antibodies used in immunostaining

Antigen (species)	Working dilution in WB	Catalog number	Company/Reference
HA-tag (rabbit)	1:1000	ab9110	Abcam
V5-tag (mouse	1:200	R960-25	Life Technologies
Tubulin β III (mouse)	1:300	ab5603	Millipore
Tuj1 (rabbit)	1:1000	802001	BioLegend
GFP (chicken)	1:1000	06-896	Millipore
Myt1L (guinea-pig)	1:1000		(Wang et al., 2007)

Table 6.2 – Secondary antibodies used in immunostaining

Antigen (species)	Working dilution in WB	Company/Reference
Alexa Fluor 488 Goat Anti-Chicken IgG	1:1000	Life Technologies
Alexa Fluor 488 Goat Anti-mouse IgG	1:1000	Life Technologies
Alexa Fluor 568 Goat Anti-rabbit IgG	1:1000	Life Technologies
Alexa Fluor 568 Goat Anti-mouse IgG	1:1000	Life Technologies
Alexa Fluor 568 Goat Anti-guinea pig IgG	1:1000	Life Technologies

9. Gene expression analysis

MEFs were plated in 6-well plates (600 000 cells/ well). Notch signalling was inhibited by adding the gamma-secretase inhibitor LY to the culture for 4 hours.

NS-5 cells were plated in 6-well plates (600 000 cells/ well).

All samples were prepared in triplicate.

10. RNA extraction

Total RNA was isolated from cells by using Trizol reagent (Invitrogen) and alcohol precipitation. Extracted RNA was purified by DNAse I (Roche) treatment followed by Rneasy column purification (RNA CleanUp protocol, Qiagen). EDTA inactivation of DNAse I step was omitted.

11. Reverse transcriptase quantitative real-time PCR (RT-qPCR)

cDNA was synthetized using the High-Capacity RNA-to-cDNA kit (Applied Biosystems) according to the manufacturers' instruction. An equal amount (500-1000 ng) of total input RNA was used on each experiment. Gene expression analysis by quantitative real-time PCR using PerfeCTa SYBR Green FastMix, ROX (Quanta Biosciences) was carried out according to the manufacturers' instructions on the CFX384 Touch™ Real-Time PCR Detection System (Biorad). The primers used are listed on Table 7. Triplicates of each biological replicate were used in the RT-qPCR. Values are normalized to β-actin expression levels and to untreated sample. Starting Quantity was calculated using the CFX Manager™ software (Biorad). Results are shown as mean ± SD of triplicate assays.

Table 7 – Primers used in expression-qPCR

Gene	Forward Primer	Reverse Primer
β-actin	CTAAGGCCAACCGTGAAAAG	ACCAGAGGCATAGGGACA
GAPDH	GGGTTCCTATAAATACGGACTGC	CCATTTTGTCTACGGGACGA
Hes1	TGAAGGATTCCAAAATAAAATTCTCTGGG	CGCCTCTTCTCCTGATAGGCTTTGATGAC
Hes5	AAGTACCGTGGCGGTGGAGAT	CGCTGGAAGTGGTAAAGCAGC
Notch1	CTGGACCCCATGGACATC	GGATGACTGCACACATTGC

12. ChIP-qPCR

12.1. Chromatin isolation from MEFs cultures

Cells were washed with PBS and fixed in PBS-Mg (1mM MgCl2 in PBS) containing 2mM Disuccinimidyl-glutarate (DSG) (Sigma-Aldrich) for 45min at RT on a rocking platform. Cells were washed with PBS and fixed in PBS-Mg with 1% formaldehyde (Sigma-Aldrich) for 10min at RT on a rocking platform. Crosslinking was quenched by addition of glycine to a final concentration of 125mM for 5min at RT. Subsequently, cells were washed twice in PBS and harvested by scraping in 1mg/mL BSA PBS (with proteinase inhibitors (Roche)). After a low speed centrifugation, cell pellets were re-suspended in SDS lysis buffer (1% SDS (Sigma-Aldrich), 10mM EDTA, 50mM Tris pH 8.0, Proteinase inhibitors) and incubated for, at least, 10min at +4 °C. Chromatin was transferred to non-sticky eppendorfs (Ambion) and sheared by sonication using a Bioruptor sonicator (Diagenode) at high power settings in 30s ON/OFF cycles at +4 °C. Centrifugation at 14 000rpm for 10min at +4 °C allowed the precipitation of cell debris and the soluble chromatin fraction on the supernatant was collected. Chromatins were

snap-frozen in liquid nitrogen and stored at -80 °C. To verify the efficiency of the sonication, an aliquot of chromatin was subjected to reverse crosslinking and Proteinase K (0.1mg/mL, Roche) digestion followed by DNA purification by phenol-chloroform extraction. Fragment size was determined by agarose gel electrophoresis.

12.2. Chromatin immunoprecipitation

Reactions were performed in non-sticky eppendorfs (Ambion) using 50-100µg of chromatin and 50µL of magnetic beads and the appropriate antibody in each ChIP reaction (Table 8). As a negative control, an IP without antibody was run in parallel. Beads were washed 5 times with washing buffers followed by one wash with TE (10mM Tris-HCl pH 8.0, 1mM EDTA) wash. Bound chromatin was eluted by incubation of the beads with elution buffer (50mM Tris-HCl pH 8.0, 10mM EDTA, 1% SDS) for 12min at 65 °C. Proteins were digested by Proteinase K (0.1mg/mL) (Roche) for 2h at 42ºC and crosslinking was reverted overnight at 65 °C. The DNA was purified performing one phenol/chloroform extraction and one chloroform:isoamyl alcohol 25:24:1 extraction followed by isopropanol precipitation and centrifugation for 20min at 14 000rpm, +4 °C. Glycogen (40µg) (Sigma-Aldrich) to facilitate the visualization of the pellet after centrifugation. For anti-RBPJ ChIP, Protein G Dynabeads (Invitrogen), high salt IP buffer (20mM HEPES pH 8.0, 2M NaCl, 2mM EDTA, 0.1% Sodium deoxycholate (NaDOC, Sigma-Aldrich), 1% Triton X-100,1mg/mL BSA, Proteinase inhibitors (Roche)) were used. Samples were subject to 3 washes with Reduced SDS Washing Buffer (50mM HEPES pH 7.6, 150mM NaCl, 2mM EDTA, 0.1% NaDOC (Sigma-Aldrich), 1% Triton X-100, 0.1% SDS), 1 wash with Reduced SDS Washign buffer high salt (Reduced SDS Washign buffer with 1M NaCl), 2 washes with LiCl buffer (10mM Tris HCl pH 8.0, 250mM LiCl, 1mM EDTA, 0.5% NP-40, 0.5% NaDOC) and 1 wash with TE buffer (10mM Tris HCL pH 8.0, 1mM EDTA).

For anti-HA ChIP, Protein G Dynabeads (Invitrogen) and high salt IP buffer were used. Sampels were subject to one wash with low-salt buffer (20mM Tris HCl pH 8.0, 150mM NaCl, 2mM EDTA, 1% Triton X-100, 0.1% SDS), one wash with high-salt buffer (20mM Tris HCl pH 8.0, 500mM NaCl, 2mM EDTA, 1% Triton X-100, 0.1% SDS) and one wash with LiCl buffer (10mM Tris HCl pH 8.0, 1mM EDTA, 1% NP-40, 1% NaDOC, 250mM LiCl).

Table 8 – Antibodies used in ChIP

Antigen (Species)	Volume used in ChIP	Catalog number	Company / Reference
RBPJ (rabbit)	7.5µL/50µL beads	5313	Cell signalling Technology
HA-tag (rabbit)	3µL/50µL beads	ab9110	Abcam

The purified DNA retrieved from the ChIP was analyzed by qPCR (primers listed on Table 9) using the standard mix protocol of PerfeCTa SYBR Green FastMix, ROX (Quanta Biosciences). Reaction was run under the following cycling conditions: 1 cycle (50ºC/ 2min; 95ºC/ 3min); 40 cycles (95ºC/ 15sec; 60ºC/ 1min); 1 cycle (95ºC/ 15sec; 60ºC/ 15sec; 95ºC/ 15sec) in ABI 7900HT (Applied Biosystems). Quantities of immmunoprecipitated DNA were calculated by comparison with a standard curve generated by serial dilutions of input DNA. Results are shown as mean ± SD of fraction of input chromatin for triplicate assays. Open reading frames (ORFs) were used as negative control regions.

Table 9 – Primers used in ChIP-qPCR

Primers	Forward Primer	Reverse Primer
Hes1 ORF (ORF1)	CACTTTCTGCCTTCTGTGGA	AGAGGATGGAGGAGTCATGG
Dll1 ORF (ORF2)	GTCTCAGGACCTTCACAGTAG	GAGCAACCTTCTCCGTAGTAG
Fbxw7 ORF (ORF2)	CTCGTCACATTGGAGAGTGG	CAGGAGCTTGGTTTCCTCAG
Hes1	GGGAAAGAAAGTTTGGGAAGT	GTTATCAGCACCAGCTCCAG
Notch1	AAGTGGGAGGGGATTAAGGT	CAGGTATTGGGTGTCGGAGT

12.3. FAIRE-qPCR

Formaldehyde-Assisted Isolation of Regulatory Elements (FAIRE) was performed as previous described (Giresi et al., 2007). Chromatin preparation was performed after a single fixation with 1% formaldehyde (Sigma-Aldrich). Three rounds of phenol/chloroform extraction were followed by isopropanol precipitation of the DNA. Quantification of genomic regions was done using a standard curve generated with de-cross-linked input chromatin by qPCR as above.

The purified DNA retrieved from the FAIRE was analyzed by qPCR (primers listed on Table 10) using the standard mix protocol of PerfeCTa SYBR Green FastMix, ROX (Quanta Biosciences). Reaction was run under the following cycling conditions: 1 cycle (50ºC/ 2min; 95ºC/ 3min); 40 cycles (95ºC/ 15sec; 60ºC/ 1min); 1 cycle (95ºC/ 15sec; 60ºC/ 15sec; 95ºC/ 15sec) in the CFX384 Touch™ Real-Time PCR Detection System (Biorad). Quantities of immmunoprecipitated DNA were calculated by comparison with a standard curve generated by serial dilutions of input DNA. Results are shown as mean ± SD of fraction of input chromatin for triplicate assays. ORFs were used as negative control regions.

Table 10 – Primers used in FAIRE-qPCR

Primers	Forward Primer	Reverse Primer
Hes1 ORF (ORF1)	CACTTTCTGCCTTCTGTGGA	AGAGGATGGAGGAGTCATGG
Dll1 ORF (ORF2)	GTCTCAGGACCTTCACAGTAG	GAGCAACCTTCTCCGTAGTAG
Hes1	GGGAAAGAAAGTTTGGGAAGT	GTTATCAGCACCAGCTCCAG

Results

1. Investigating the Notch signalling activity in Mouse Embryonic Fibroblasts (MEFs)

1.1. Generation of MEFs from Transgenic Notch Reporter (TNR) mice

Notch signalling activity in mouse embryonic fibroblasts (MEFs) has been implicated with promoting cell cycle arrest and apoptosis (Ishikawa et al., 2008; Liu et al., 2012), but it is still unclear to which extent the endogenous Notch pathway is active in this cellular context. To study the activity of the endogenous Notch signalling I made use of the Transgenic Reporter mice line (TNR). These mice express Enhanced Green Fluorescent protein (eGFP) under the control of 4 tandem copies of the RBPJ binding site consensus sequence. When Notch is activated, the NICD-RBPJ complex forms and activates eGFP expression (Figure 4B). I therefore isolated MEFs from TNR mice and established TNR-MEF cell cultures (Figure 4A).

Since cell contact promotes the activation of the canonical Notch signalling pathway, MEFs were cultured at different densities (120, 240, 360 cells/µL) and tested for the levels of eGFP expression by immunostaining against eGFP. However, eGFP staining was not detected in any of the cultures tested (data not shown).

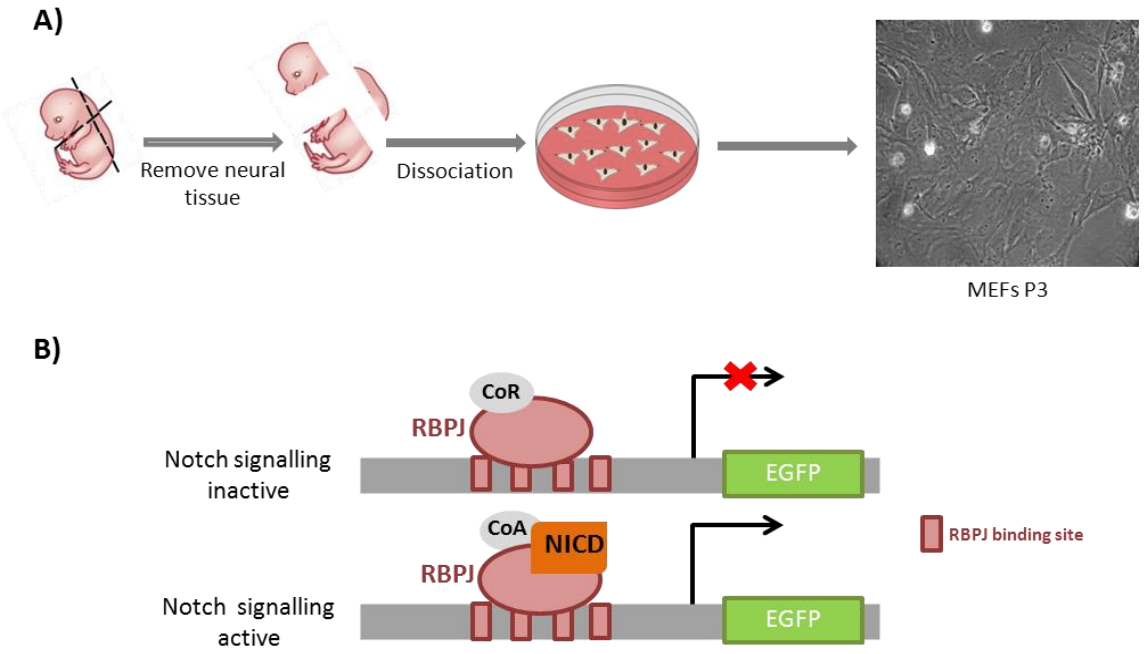

Figure 4 – MEFs production protocol and TNR mice Notch activity reporter. (A) Scheme depicting the

general production of mouse embryonic fibroblasts (MEFs) and live imaging of wild-type MEFs culture from 3rd passage (P3). **(B)** Transgenic Notch Reporter (TNR) present in TNR mice, in which four tandem RBPJ binding sites mediate Notch signalling of the expression of eGFP.

Although this could be indicative of no/low Notch signalling activity, a more definite conclusion will require testing the functionality of the transgenic system by ectopic expression of Notch activators in TNR MEF cultures.

1.2. Evidence for very low levels of Notch signalling in MEFs

Given that the reporter failed to provide an indication of Notch activity in MEFs, it is possible that Notch activity is much lower in MEFs than in other cell types. To investigate this, I compared the mRNA levels of known Notch targets in cultured NS/PCs (NS-5 cells), known to have high levels of Notch activity, with the correspondent levels in wild type MEFs. In fact, the expression analysis through qPCR quantification shows that Notch targets *Hes1* and *Notch1* are expressed at the same order of magnitude in wild type MEFs and NS-5 cells in culture. This is equally observable in the housekeeping genes β-Actin and GAPDH. In contrast, the mRNA levels for Hes5, a target that is widely used as a read-out of Notch signalling activity (Basak and Taylor, 2007; Lugert et al., 2010), is 1000 times lower in wild type MEFs when compared to those measured for NS-5 cells in culture (Figure 5A). To assess for Notch activity dependency, wild type MEFs were incubated with an inhibitor of Notch signalling, the γ-secretase inhibitor LY-411575 (herein referred to as LY). Levels of expression of Hes1 and Hes5 were measured by qPCR and compared between two conditions, with and without LY. While Hes5 expression is downregulated 2-fold in presence of LY (Figure 5B), no alteration of Hes1 expression is detected (Figure 5C).Overall, these results suggest that Hes5 is expressed at very low levels in MEFs and Hes1 is highly expressed in MEFs, with no indication of Notch signalling being involved.

1.3. RBPJ binds to the *Hes1* proximal promoter in MEFs

The previous results show that *Hes1 and Hes5* have different expression levels in MEFs. To determine if the expression levels are a result from different accessibility to their promoter region I performed a FAIRE-qPCR of the proximal promoter regions of *Hes1* and *Hes5* (Figure 6A). High enrichment for nucleosome-depleted DNA of the *Hes1* proximal promoter region was found. The contrary was observed for the *Hes5* proximal promoter region (Figure 6B). The two promoter regions where compared to two negative control regions. The results demonstrate that difference in expression of *Hes1* and *Hes5* is related to differences in their respective promoter regions accessibility.

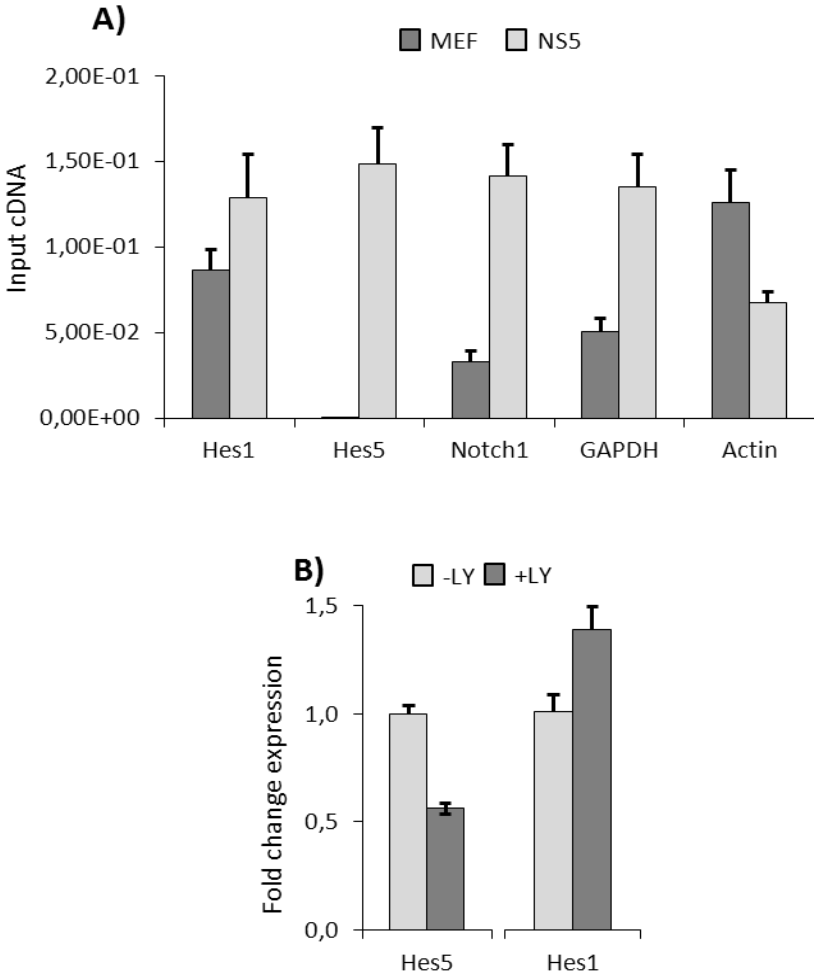

Figure 5 – Hes1, but not Hes5, is expressed in MEFs. **(A)** Comparative expression analysis of Hes1, Hes5, Notch1, GAPDH and β-Actin in MEFs and NS-5 cells; **(B)** Gene expression analysis of Hes5 and Hes1 in MEFs before (-LY) or after (+LY) treatment with ɣ-secretase inhibitor LY-411575 by expression real-time PCR. Mean ± SD of triplicate assays are shown.

In NS/PCs, *Hes1* is regulated by Notch signalling through the activity of RPBJ-NICD activator complex. RBPJ regulates *Hes1* through binding to three consensus binding sequences located in *Hes1* proximal promoter region (Figure 2B) (Iso et al., 2003). To determine if endogenous RBPJ binds to the *Hes1* proximal promoter region, I performed chromatin immunoprecipitation (ChIP) with antibody against RBPJ, followed by qPCR (Figure 7A). Different sonication times (10, 20 and 30minutes) were initially tested for the chromatin extracted from wild type MEF cultures, indicating an ideal sonication time of 30 minutes for chromatin fragments ranging in size between 100-400bp (Figure 7B). ChIP-qPCR results demonstrate a strong enrichment of RBPJ to the *Hes1* proximal promoter region, as compared with the negative control regions (Figure 7C).

Overall, both FAIRE- and ChIP-qPCR results are consistent with the proximal promoter region of *Hes1* being accessible for transcription factor binding.

2. MyT1L counteracts Notch activation of the *Hes1* promoter by direct DNA-binding

2.1. Generation of a tagged version of MyT1L

With the aim of studying binding of MyT1L to its putative target genes in MEFs by ChIP, I generated a tagged version of MyT1L to increase ChIP efficiency. The influenza hemagglutinin tag (HA tag) was fused to MyT1L C-terminus. This was performed by PCR amplification of a fragment using pCAG-Myt1L as a template (Figure 8A). The amplification also included an *EcoR*I site, a step required for subsequent sub-cloning in to a lentiviral vector. To confirm expression, HEK293T cells were transfected with two different clones of pCAG-MyT1L-HA. Expression of both constructs was confirmed in a western blot by the presence of a protein corresponding to the expected molecular weight of approximately 133kDA (Figure 8B).

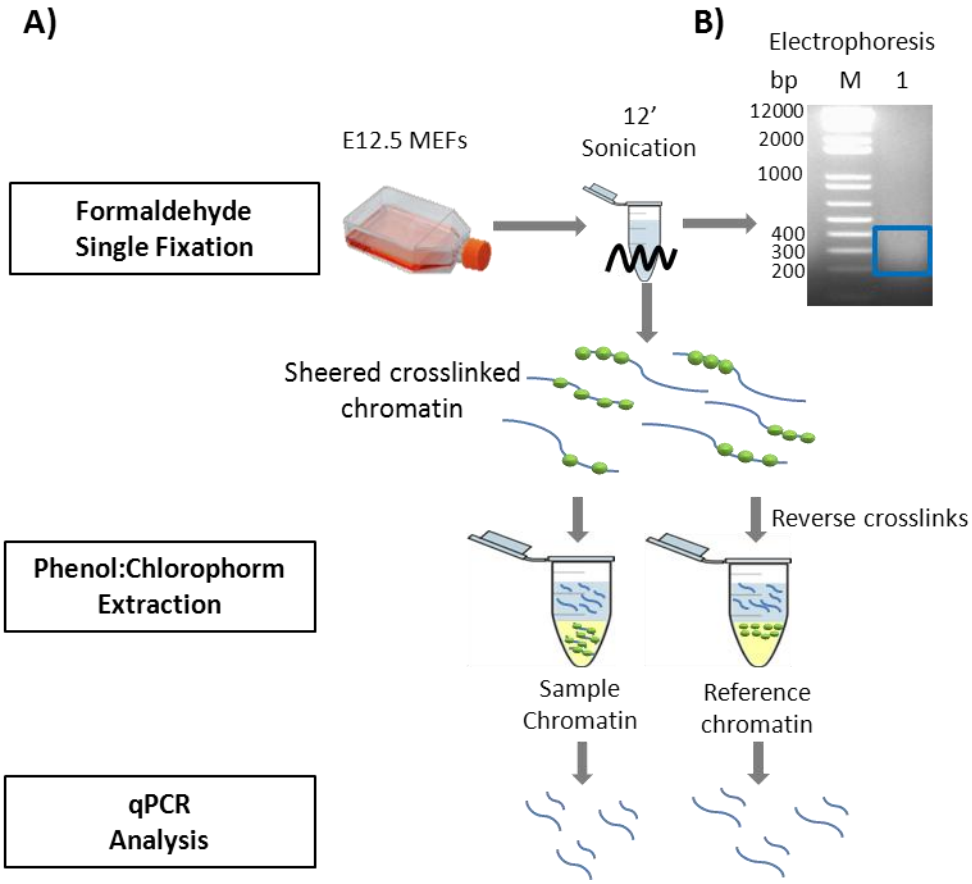

(Figure continues next page)

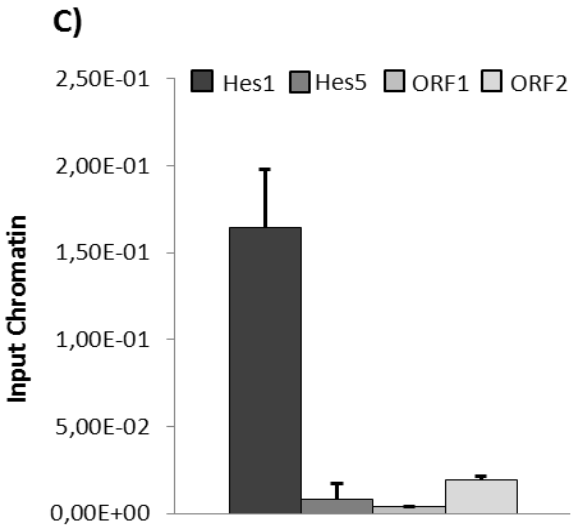

Figure 6– Chromatin is accessible in the *Hes1* proximal promoter region in MEFs. (A) Scheme depicting of the FAIRE protocol followed by real-time PCR. **(B)** Analysis of the DNA fragments size by electrophoresis after sonication of the chromatin. Blue rectangle indicates chromatin fragments. **(C)** Quantification of nucleosome-depleted chromatin at *Hes1* and *Hes5* proximal promoter region by FAIRE-qPCR using chromatin extracted from MEFS derived from E12.5 wild-type mice. Two negative control regions within the gene open reading frame (ORF) were tested (ORF1-Hes1; ORF2-Dll1). Mean ± SD of triplicate assays are shown.

In order to assess the functionality of the fusion protein, a Reporter Gene Assay (RGA) was performed in transfected P19 cells, using a construct containing the luciferase gene under the regulation of the *Hes1* proximal promoter region. This vector was co-transfected with expression vectors encoding activated Notch1 (aN1) (a dominant active version of the Notch1 receptor), MyT1L wild type (MyT1L-WT) and MyT1L-HA. As expected, aN1 upregulates the activity of the Hes1 promoter by 20-fold (Figure 8C), while in presence of either MyT1L species this upregulation is significantly reduced to less than 5-fold. This result indicates that the MyT1L-HA construct is able to downregulate the Hes1 promoter to the same extent of the MyT1L-WT.

Overall, these experiments indicate that the MyT1L-HA fusion construct is functional and expressed with the correct molecular weight.

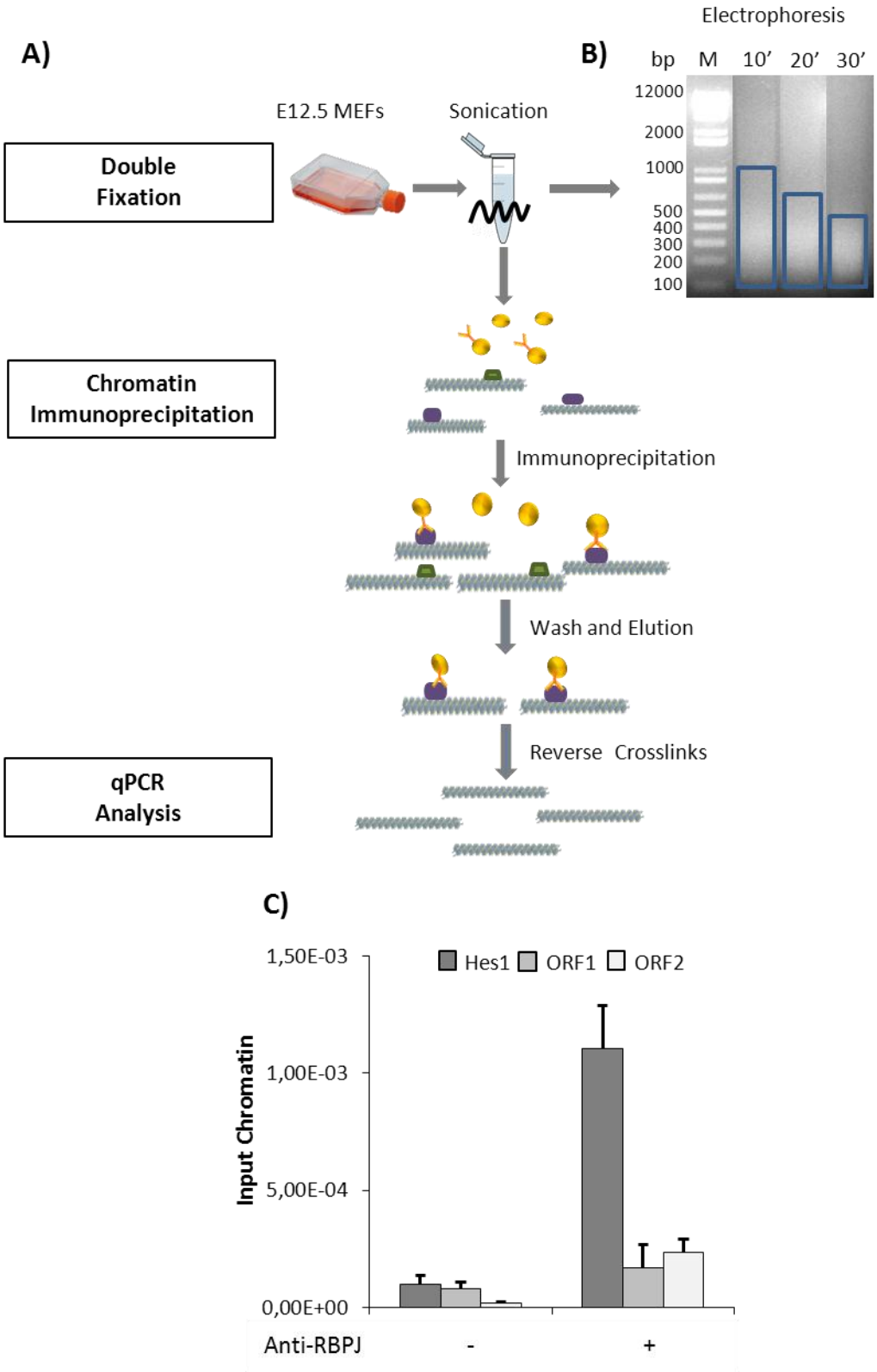

Figure 7 – MEFs have endogenous RBPJ binding to the *Hes1* proximal promoter region. **(A)** Scheme depicting the chromatin immunoprecipitation (ChIP) protocol followed by real-time PCR. **(B)** Analysis of the DNA fragments size (blue rectangles) by electrophoresis of the chromatinafter different sonication times. Blue rectangle indicates chromatin fragments. **(C)** Analysis of endogenous RBPJ binding to the

Hes1 proximal promoter region by ChIP-qPCR, using chromatin extracted from MEFs derived from E12.5 mice wild-type. Analysis of the chromatin was made with (+) and without (-) antibody against RBPJ. Two negative control regions within open reading frames (ORFs) were tested (ORF2-Dll1; ORF3-Fbxw7). Mean ± SD of triplicate assays are shown.

2.2. Comparing MyT1L and MyT1 activities in the *Hes1* proximal promoter region

MyT1 is a zinc-finger transcription factor paralog to MyT1L. Work in our laboratory found that MyT1 strongly represses the Notch activation of the *Hes1* proximal promoter. In order to compare the ability of MyT1L and MyT1 to inhibit the *Hes1* proximal promoter, I performed a RGA where different ratios of transcription factors and NICD were used. Since NICD is more efficient than aN1 in activating the *Hes1* proximal promoter, I chose to use this vector. As expected, NICD upregulates the *Hes1* promoter by 60-fold (Figure 9). In contrast, when cells also express MyT1L or MyT1 the NICD-dependent activity of the *Hes1* promoter activation is strongly reduced at all tested ratios (Figure 9).

The results suggest a redundant function between MyT1L and MyT1 in counteracting Notch activity in the *Hes1* proximal promoter. Interestingly, MyT1L repression was more efficient when competing with higher concentrations of NICD, suggesting a stronger affinity to the *Hes1* proximal promoter region.

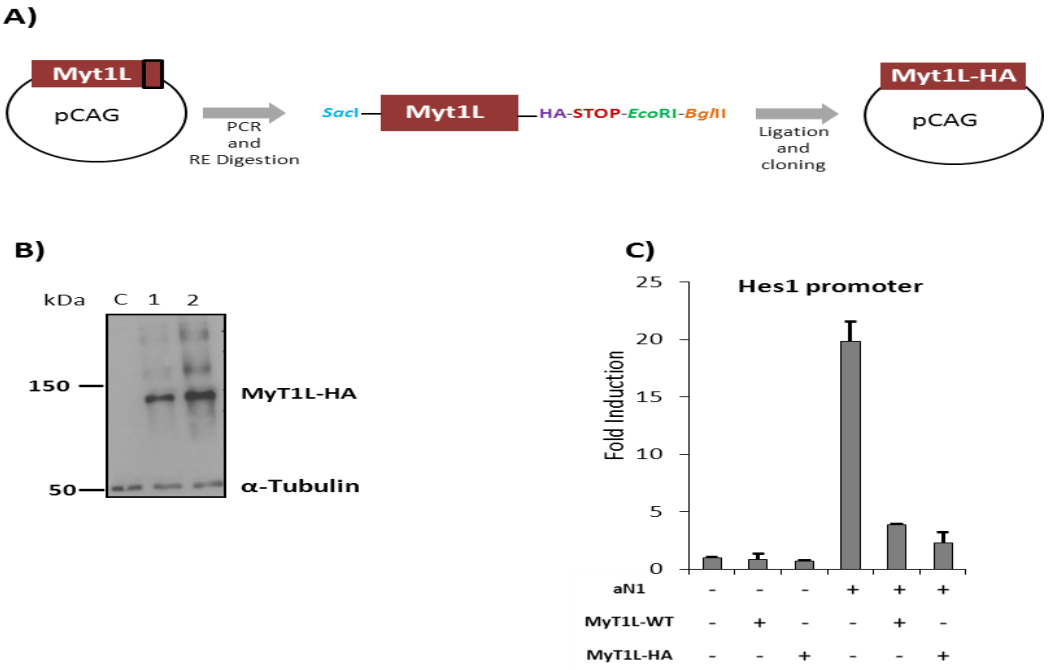

Figure 8 – MyT1L-HA downregulates the Notch activated *Hes1* proximal promoter. **(A)** Scheme depicting the pCAG-MyT1L-HA plasmid sub-cloning. Black rectangle indicates the amplified fragment from the MyT1L wild type. **(B)** Analysis of protein size of MyT1L-HA expressed from two distinct clones of pCAG-MyT1L-HA (1-2) by Western blot. **(C)** Reporter gene assays in P19 cells co-transfected with control, Activated Notch (aN1), MyT1L and/or MyT1L-HA expression vectors and a reporter construct

expressing luciferase under the control of Hes1 proximal promoter region. Mean ± SD of triplicate assays are shown.

2.3. MyT1L binds the *Hes1* proximal promoter region in MEFs

Sequence analysis of the *Hes1* proximal promoter showed the existence of three MyT1 binding sites (Figure 2B). In fact, previous work in our laboratory demonstrated that MyT1 directly binds to the MyT1 binding sites region of the *Hes1* proximal promoter in NS/PCs. Since MyT1L is structurally similar to MyT1 and given the previous results with RGAs, one could expect that MyT1L also binds to the same region of the *Hes1* proximal promoter when ectopically expressed in MEFs. To verify this I performed a ChIP-qPCR against MyT1L-HA. Chromatin was extracted from MEF cultures expressing MyT1L-HA upon lentiviral delivery. The chromatin extraction protocol was previously optimized in order to have a maximum of number of MEFs expressing MyT1L-HA with the minimum addition of lentivirus. The protocol was downscaled from 3x T150 flasks to a T25 flask. Optimization of the protocol demonstrated that extracted chromatin from a T25 flask was equally sonicated as the chromatin extracted from T75 and T150 flasks (Figure 10A).

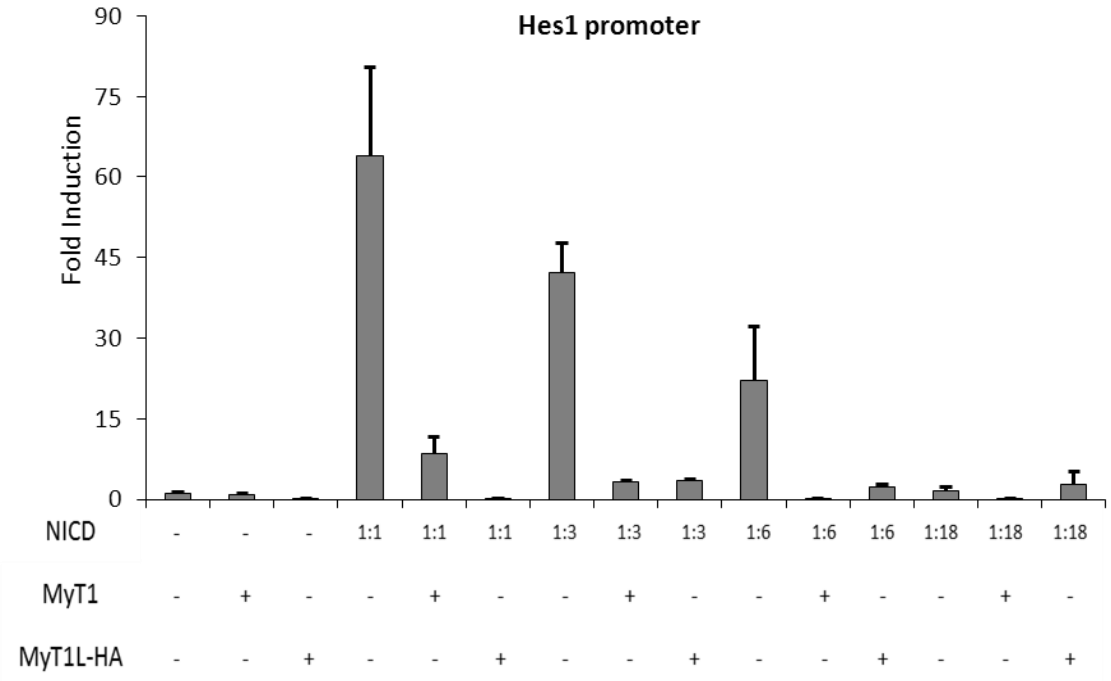

Figure 9 – MyT1L and MyT1 counter act Notch activation of *Hes1* proximal promoter. Reporter gene assays in P19 cells co-transfected with control, Notch Intracellular Domain (NICD), MyT1 and/or MyT1L-HA expression vectors and a reporter construct expressing luciferase under the control of Hes1 proximal promoter region. The different NICD:MyT1 or NICD:MyT1L-HA are depicted in the figure. Mean ± SD of triplicate assays are shown.

Cultured MEFs were infected with a mix of lentiviruses combining a MyT1L-HA with the reverse tetracycline transactivator (rtTA). The MyT1L-HA lentivirus encapsulates the TetON-FUW-Myt1L-HA construct sub-cloned from the previously generated pCAG-Myt1L-HA plasmid. The expression of MyT1L-HA was induced by the addition of Doxycycline (DOX) (Figure 10B) and chromatin extracted two days after the induction (Figure 10C). The ChIP-qPCR was performed with a ChIP grade antibody direct against the HA tag. MEFs infected with MyT1L-HA show strong enrichment of MyT1L-HA in the Hes1 promoter region, as compared with two negative control regions (Figure 10D). The same was not observed in uninfected MEFs. Additionally, MyT1L-HA binding was also detected at a regulatory region in the vicinity of the *Notch1* gene. Previous work in our laboratory showed binding by MyT1 in this regulatory region of the *Notch1* gene in NS/PCs.

Overall, these results show that MyT1L can bind to the *Hes1* promoter region in MEFs two days after being ectopically expressed suggesting a potential role for MyT1L in regulation of *Hes1* expression in MEFs.

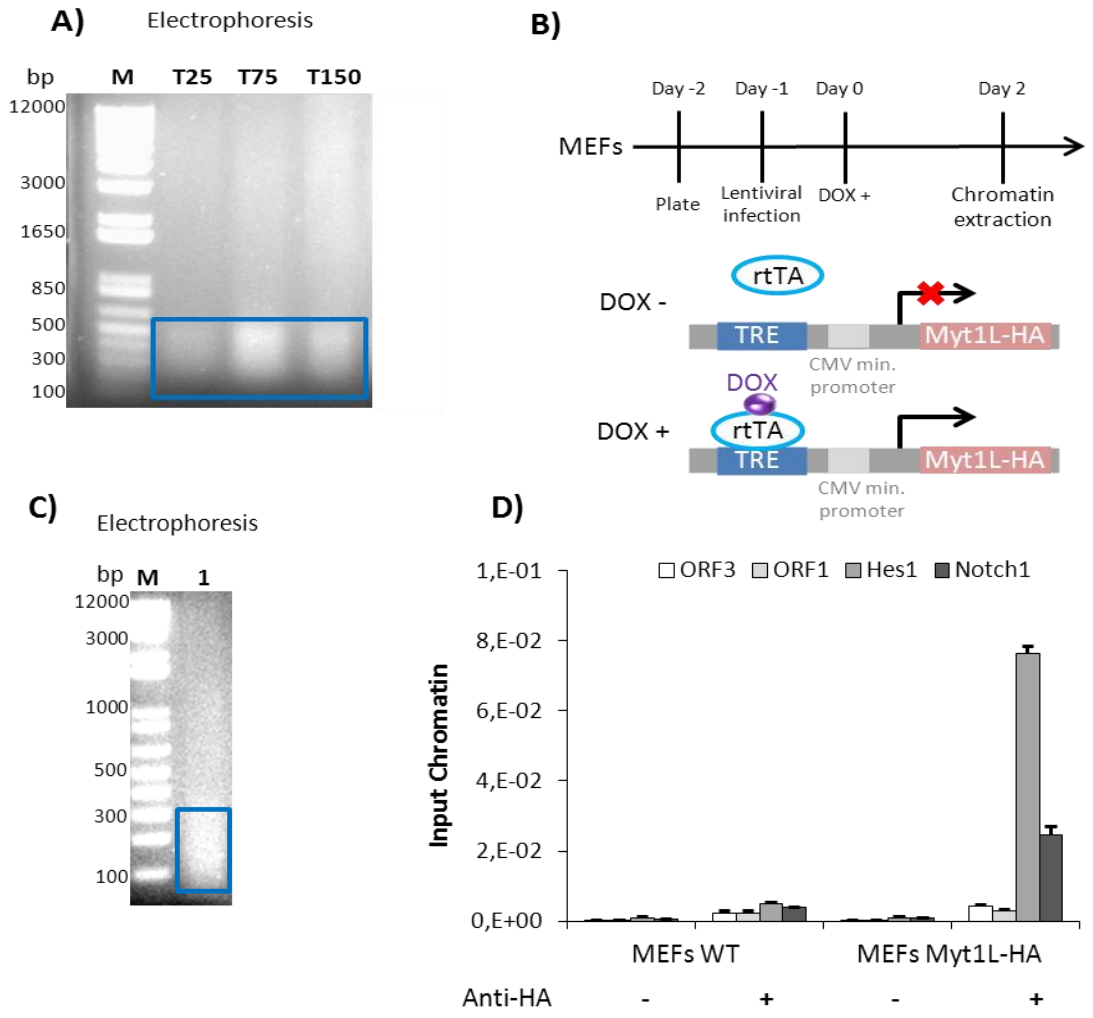

Figure 10 – MyT1L binds to the *Hes1* and *Notch1* proximal promoter regions. (A) Analysis of the chromatin fragments size after 14 minutes sonication by electrophoresis. Chromatin was extracted from

MEFs cultured in T25, T75 or T150 flasks. Blue rectangle indicates chromatin fragments. **(B)** Scheme depicting the experiment in which MEFs infected with TetON-FUW MyT1L-HA were induced by DOX and harvested for chromatin extraction and ChIP. **(C)** Chromatin fragment size analysis by electrophoresis after 14 minutes sonication of the chromatin previously extracted. The chromatin was extracted from MEFs culture in T25 flasks. Blue rectangle indicates chromatin fragments. **(D)** Analysis of MyT1L-HA binding in the Hes1 proximal promoter region and Notch1 promoter region by ChIP-qPCR in chromatin extracted from MEFs wild-type (without lentivirus infection) and MEFs MyT1L-HA (with Myt1L-HA lentivirus infection). Both chromatins were tested with and without anti-HA tag. Two negative control regions within open reading frames (ORFs) were tested (ORF1-Hes1; ORF3-Fbxw7). Mean ± SD of triplicate assays are shown.

3. Establishment of a method to reprogram fibroblasts into induced Neurons (iN cells)

3.1. Optimization of the lentiviral infection protocol

In order to establish a reprogramming protocol to convert MEFs into iN cells, it is necessary to first optimize the efficiency of lentiviral infection in this cell type. I determined the optimal amount of Polybrene, a polymer that enhances the ability of the virus to infect, at three different concentrations, 1, 4 and 8 µg/mL. Polybrene was added to a lentivirus mix containing the vectors for V5-Ascl1, rtTA and GFP (A-1F Mix) (Figure 11A) in MEF cultures. After DOX induction during two days, immunocytochemistry was performed against the V5 tag. The number of V5+ cells increases with the increase of polybrene concentration (Figure 11B, C). Infected MEFs with no induction were used as a control.

Following the previous result, the minimum volume of virus stock needed to have high infection levels and low cell death was tested. The experiment included conditions with different volumes (2.5, 10, 15, 20 µL) for the A-1F Mix and the 1F Mix with the MyT1L-HA lentivirus (M-1F Mix) (Figure 12A). The infection was performed with 8µg/mL of Polybrene. MEFs were infected with Empty, rtTA and GFP lentivirus (Control Mix) to control for lentivirus infection effects in MEFs. The results show a maximum of cell infection from both factors around the 10%-12% (Figure 12C, E). The minimum volume to reach this value for MyT1L-HA lentivirus is 10 µL. V5-Ascl1 lentivirus produces the same maximum percentage of cell infection that is observed with MyT1L-HA infection. No increase was observed when further increasing the viral volume (15 or 20 µL, Figure 12B, D). It was not possible to obtain data for the 10 µL V5-Ascl1 lentivirus infection due to loss of sample.

The addition of 8µg/mL of Polybrene and 10 µL of virus from each factor results in an infection rate of ≈10% of the cells in culture. Although low, this can still be considered a

significant rate of infection and these conditions were therefore used in the subsequent experiments.

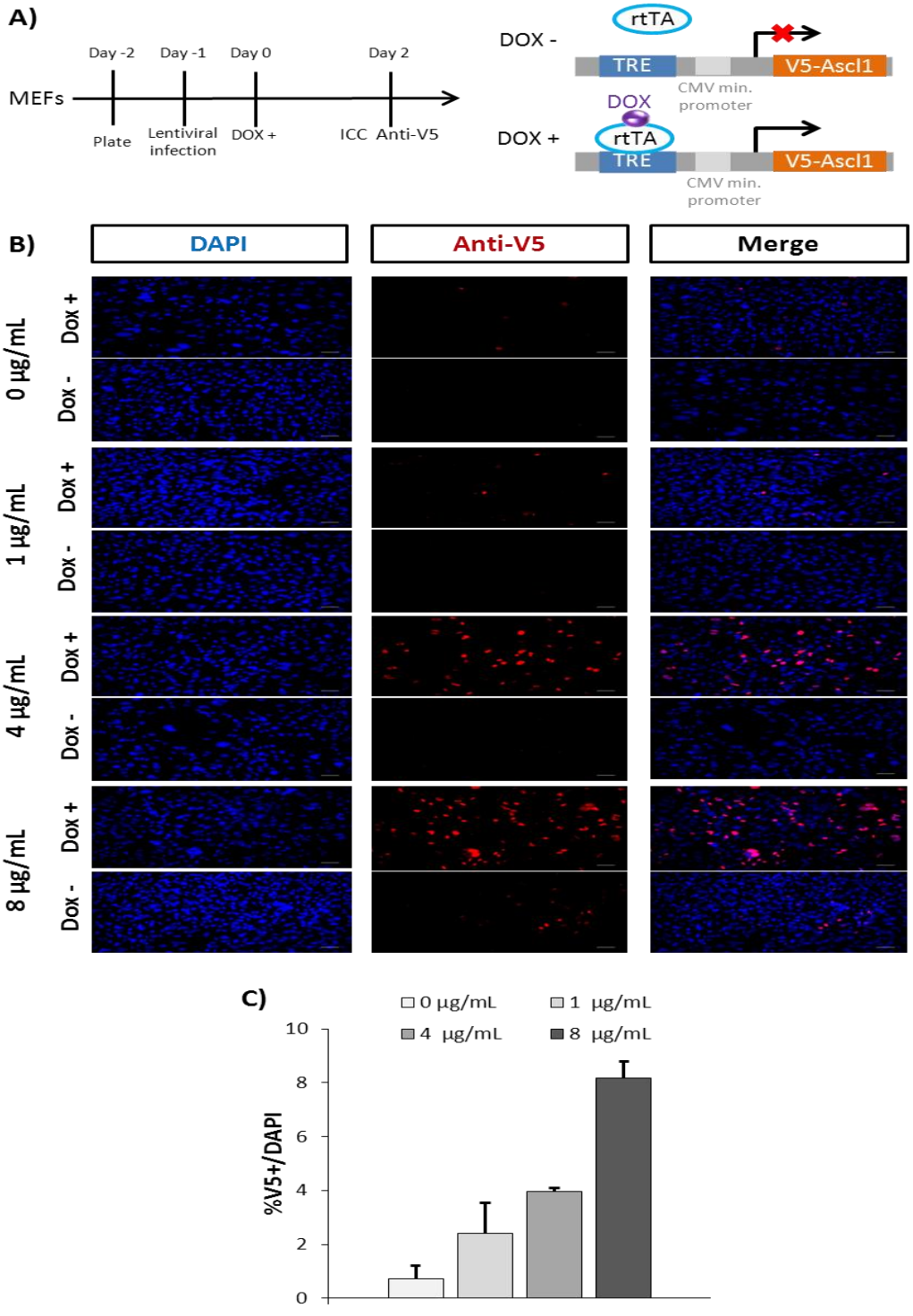

Figure 11 – Higher concentrations of polybrene correlate with higher infection rate. (A) Scheme depicting experiment in which MEFs were infected with V5-Ascl1 inducible lentiviruses with different concentration of polybrene. Infection rate was assessed by expression of V5-Ascl1 induced after addition of DOX. **(B)** Analysis by immunocytochemistry for the V5-tag upon infection with V5-Ascl1 expressing lentivirus with different concentration of polybrene (0,1 , 2, 4 and 8µg/mL) 2 days after

addition of DOX. Control MEFs were infected with Ascl1-V5 lentivirus but were not induced. Scale bar: 50 µm. **(C)** Histogram represents the percentage of MEFs infected with V5-Ascl1 lentivirus (V5+/DAPI) with each concentration of polybrene. Data presented as the mean ± SD for 10 randomly selected fields for each condition.

3.2. Ascl1 and Ascl1/MyT1L-dependent reprogramming of MEFs

It has been previously demonstrated that the ectopic expression of Ascl1 in MEFs is sufficient to promote neuronal reprogramming of these cells, even in the absence of other known reprogramming factors (Chanda et al., 2014; Vierbuchen et al., 2010). I therefore applied a single-factor reprogramming protocol with Ascl1 expression to our MEFs in the optimized conditions described above. MEFs cultures were therefore infected with the A-1F Mix or the Control Mix. One day after infection V5-Ascl1 expression was induced with DOX. Cells were transferred two days later to neuronal differentiating medium (N3 medium). Cultures were then collected for immunostaining against Tuj1 at 7, 14 and 21 days post-induction (Figure13A). At 7 days post-induction, some of the cells expressing V5-Ascl1 also express Tuj1, whilst none of the control cells show Tuj1 staining (Figure 13B). The percentage of Tuj1+ cells was approximately 3% (Figure 13C), an efficiency considerably lower than the one that has been reported in the literature (Chanda et al., 2014; Vierbuchen et al., 2010). Also, the observed Tuj1+ cells display an immature morphology and lacked neurites or extensions. It was no possible to observe reprogrammed cells in cultures from 14 days post-induction and onwards as these did not survive the long incubation periods.

Since the combination of Ascl1 with MyT1L has been shown to be more effective than single-factor reprogramming in MEFs, I proceed to co-infect the cells with lentivirus mix combining V5-Ascl1, rtTA, and either MyT1L-HA (HA-2F MIX) or MyT1L-WT (WT-2F Mix).Cells were also infected with A-1F Mix. In order to increase the survival rate observed 7 days post-induction in N3, this neuronal differentiating medium was substituted by the N2B27 medium. Induction and change of medium were performed at the same time points described above. Cells were collected for immunostaining against Tuj1 7 to 14 days-post induction (Figure 14A). At 7 days post-induction, some of the cells expressing V5-Ascl1, and V5-Ascl1 with MyT1L-HA or –WT also expressed Tuj1, whereas none of the control cells (infected with Control Mix) show Tuj1 staining (Figure 14B). The percentage of Tuj1+ cells from the cultures infected with A-1F Mix was approximately 3.5% (Figure 14C). The percentage of Tuj1+ cells for cultures with HA- and WT-2F Mix was 1% and 2.5% respectively. Samples infected with the 2F Mix presented a much higher rate of cell death (Figure 14C) than observed in other conditions. As in the previous experiment, the immature morphology of Tuj1+ cells indicates either premature cell death or a delayed development into mature neurons (Figure 14B).

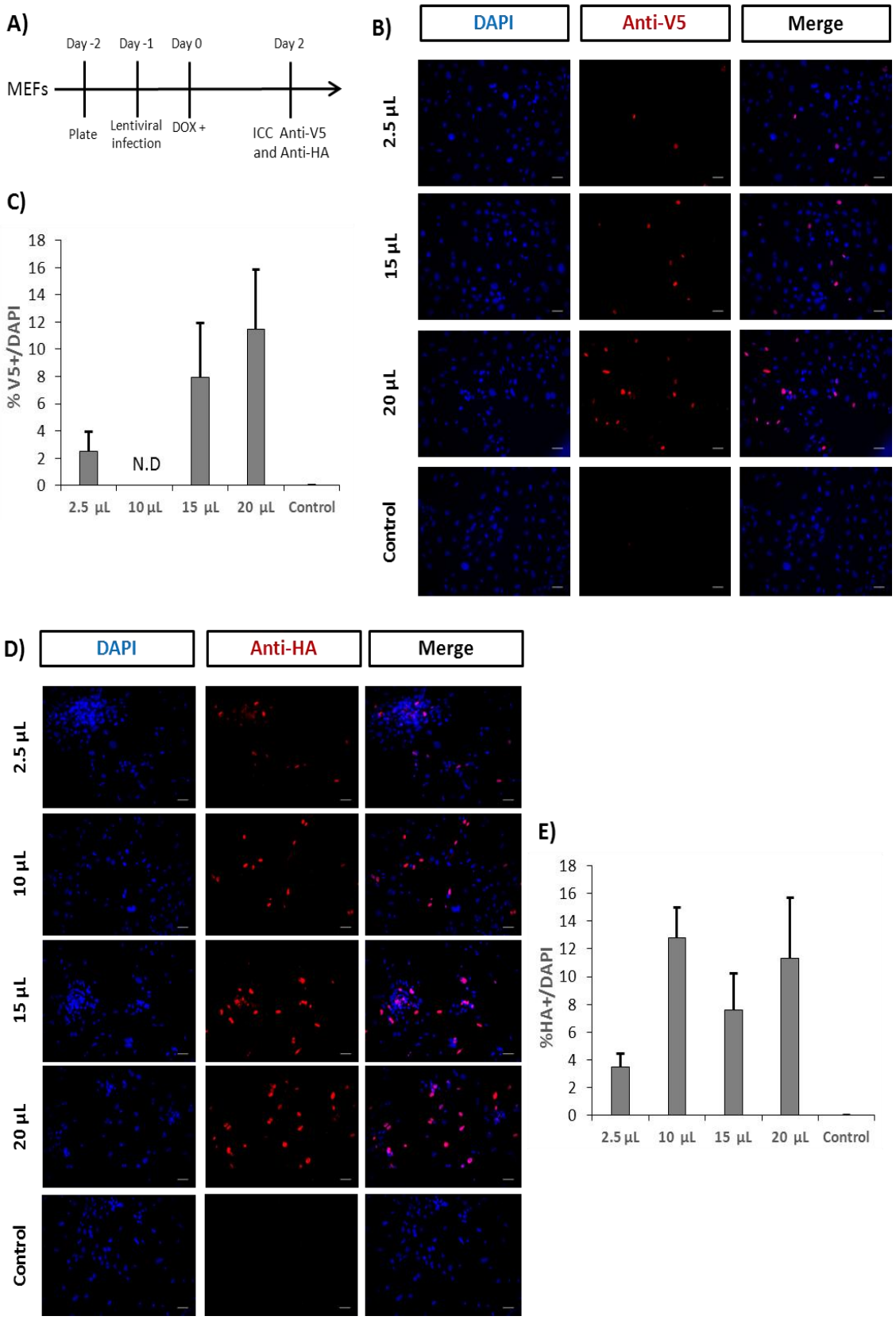

Figure 12 – Higher amount of virus result in higher infection rates but not above ≈12%. (A) Scheme depicting experiment in which MEFs were infected with V5-Ascl1 and MyT1L-HA inducible lentiviruses with different volumes from virus stock. Infection rate was assessed by expression of V5-Ascl1 and

MyT1L-HA induced after addition of DOX. **(B, D)** Analysis by immunocytochemistry for the anti-V5 tag and anti-HA tag upon infection with different volumes of V5-Ascl1, MyT1L-HA and Empty lentivirus (Control) stock. MEFs cultures were collected for analysis 2 days after induction with DOX. Scale bar: 50 µm. **(C, E)** Histogram represents the percentage of MEFs infected with V5-Ascl1 lentivirus (V5+/DAPI), MyT1L-HA lentivirus (HA+/DAPI) and Control, for each volume of lentivirus stock. Data presented as the mean ± SD for 10 randomly selected fields for each condition.

The alteration of neuronal differentiating medium did successfully prolong the survival of cells beyond 7 days post-induction, but did not increase significantly the percentage of Tuj1+ cells. No Tuj1+ cells were found at 14 day post-induction, and very few cells remained alive at this time point.

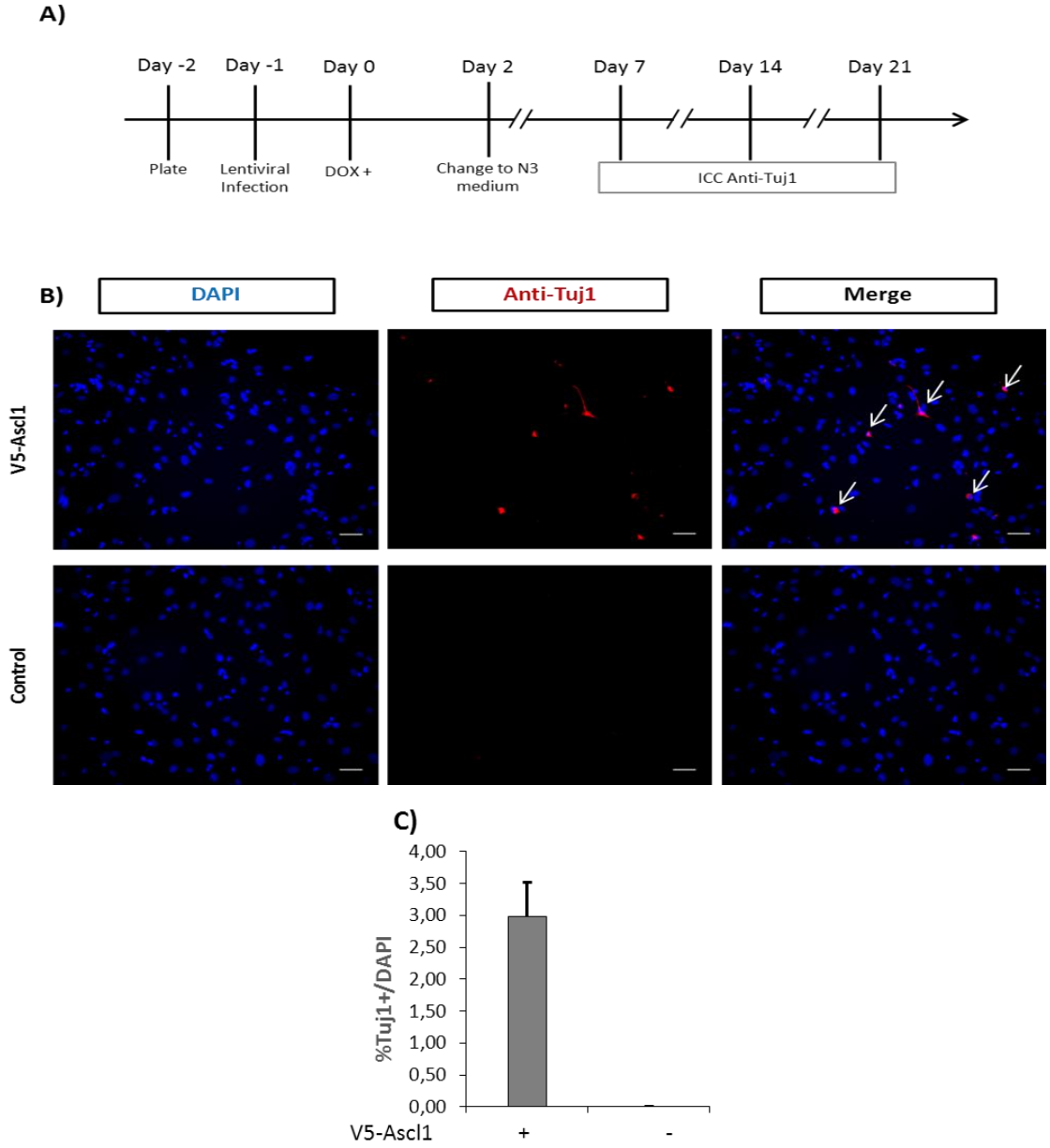

Figure 13 – MEFs reprogramming to iN cells with overexpression of Ascl1. **(A)** Scheme illustrating the experiment in which MEFs were reprogrammed to iN cells by infection with V5-Ascl1 inducible

lentivirus. **(B)** Immunocytochemical analysis for the neuronal marker Tuj1 upon infection with V5-Ascl1 lentivirus or Empty lentivirus (Control) 7 days post induction. White arrows indicate the Tuj1+ cells. Scale bar: 50 µm. **(C)** Histogram represents the percentage of Tuj1+ cells (Tuj1+/DAPI) 7 days post-induction of V5-Ascl1 expression in MEFs infected with V5-Ascl1 ("+") or Empty ("-") lentiviruses. Data presented as the mean ± SD for 10 randomly selected fields for each condition.

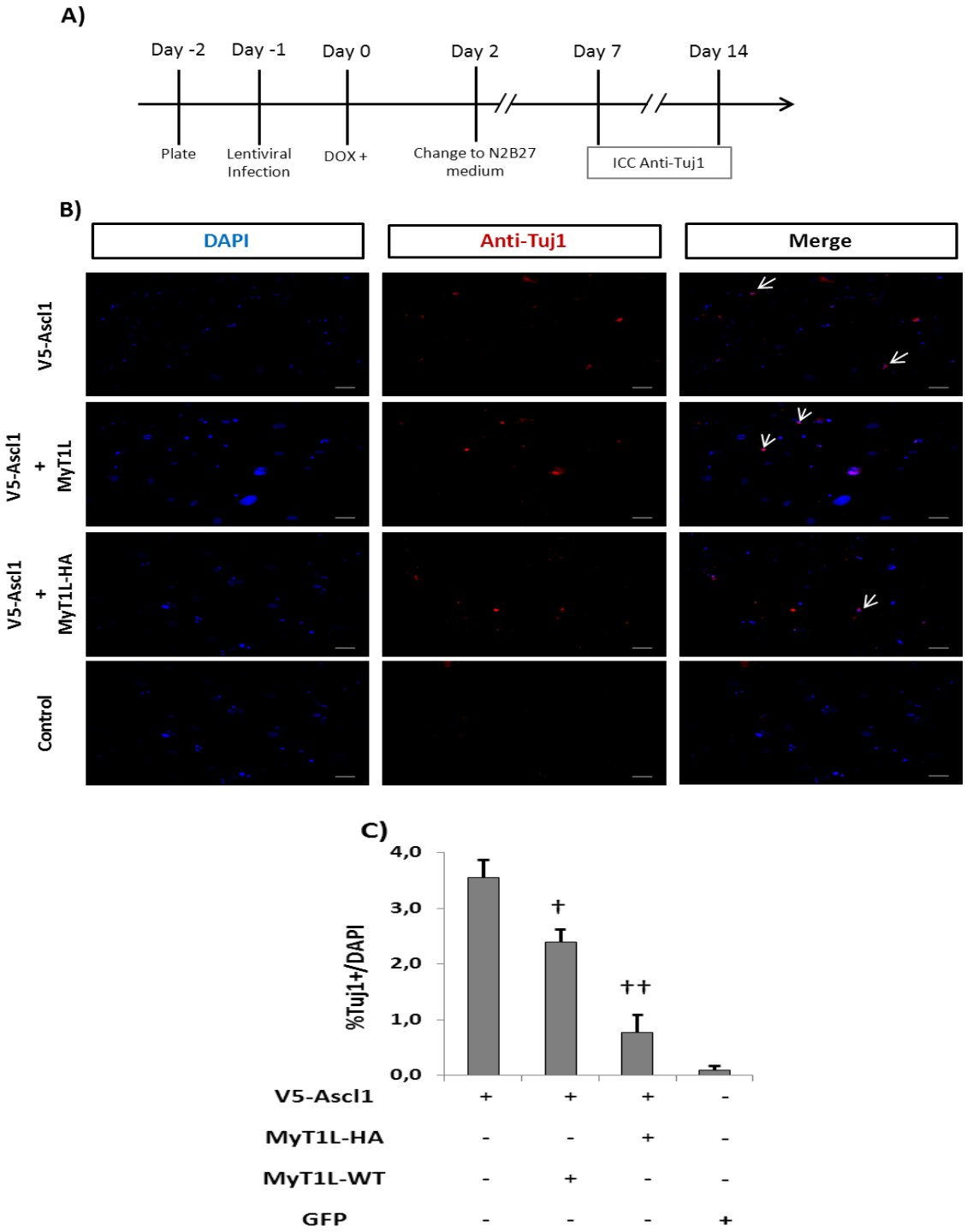

Figure 14 – MEFs reprogramming to iN cells with overexpression of Ascl1 and Ascl1 plus MyT1L-WT/HA. **(A)** Scheme illustrating the experiment in which MEFs were reprogrammed to iN cells by infection with V5-Ascl1 inducible lentivirus alone or in combination with MyT1L-WT/HA inducible

lentiviruses. **(B)** Immunocytochemical analysis for Tuj1 upon infection with V5-Ascl1 lentivirus without and with MyT1L-HA or MyT1L-WT 7 days post induction. Empty lentivirus infection was used as control. White arrows indicate the Tuj1+ cells. Scale bar: 50 µm. **(C)** Histogram represents the percentage of Tuj1+ cells (Tuj1+/DAPI) 7 days post-induction of V5-Ascl1 expression alone or in combination with MyT1L-WT/HA expression in MEFs. Data presented as the mean ± SD for 30 consecutive fields for each condition. ✝ represents the rate of cell death.

Discussion

MyT1L was described to have a late function in Ascl1-dependent reprogramming, mainly driving the maturation process of iN cells, increasing their morphological complexity and their electrophysiological properties (Pang et al., 2011; Pfisterer et al., 2011; Vierbuchen et al., 2010). The work here shows that ectopically expressed MyT1L can bind to DNA in MEFs as early as 2 days after MyT1L induction. Specifically, it is shown that MyT1L can bind to the proximal promoter of *Hes1* and repress its activity. This suggests that one of the roles of MyT1L in Ascl1-dependent reprogramming of MEFs into neurons is the transcriptional derepression of Ascl1 targets via inhibition of endogenous Hes1 expression.

Although a couple of previous studies have implicated Notch signalling in the promotion of cell cycle arrest and apoptosis of MEFs (Ishikawa et al., 2008; Liu et al., 2012), it is still unclear to which extent the endogenous Notch pathway is active in this cellular context. To assess the level of activity of Notch signalling in MEFs, I measured the levels of expression of its downstream targets, *Hes1* and *Hes5*. Surprisingly, the expression of Hes1 in MEFs is at the same order of magnitude of the levels measured for culture NS/PCs, which display high levels of Notch activity. However, treatment with the γ-secretase does not affect Hes1 expression, suggesting that the Notch pathway is not the main regulator of Hes1 expression in MEFs. The *Hes5* promoter is often used as a reporter of Notch signalling *in vivo* where its expression levels are often considered a readout of Notch activation (Basak and Taylor, 2007; Lugert et al., 2010). In contrast to Hes1, the expression of Hes5 is found at very low levels in MEFs when compared to those found for in cultured NS/PCs. Overall, this suggests that Notch signalling is not strongly active in MEFs.

Hes1 is regulated by the Notch effector RBPJ in NS/PCs (Iso et al., 2003; Louvi and Artavanis-Tsakonas, 2006). Sequence analysis of *Hes1* proximal promoter region shows the presence of three RBPJ binding sites (Figure 2B) (Iso et al., 2003). I observed RBPJ enrichment in the RBPJ binding sites region of the *Hes1* promoter in MEFs. RBPJ regulation is dependent of Notch activity, as it needs the interaction with the cleaved Notch receptor, NICD, to form an activator complex. On the other hand, when Notch activity is low RBPJ acts as a repressor (Castel et al., 2013). Since the results suggest low activity of Notch signalling, RBPJ may be acting as a repressor in MEFs. I show that Hes1 is highly expressed in MEFs, suggesting that RBPJ repression of Hes1 in these cells may be in competition with activating mechanisms which are independent of Notch activity. In mouse fibroblasts, Hes1 expression is known to be controlled by other pathways independent of Notch activity. Such pathways include the Sonic-Hedgehog pathway and the JAK-STAT signalling pathway (Ingram et al., 2008; Yoshiura et al.,

2007). The Sonic-Hedgehog regulation of *Hes1* was shown to be independent of γ-secretase-mediated Notch cleavage (Ingram et al., 2008). Since the transcription factor Hes1 regulates negatively its own expression, stabilization of Hes1 protein by inhibition of JAK-STAT signalling results in a sustained expression of Hes1 (Yoshiura et al., 2007). Moreover, in human intestinal tumorigenesis, the Wnt/β-catenin signalling was shown to up-regulate Hes1 expression independently of Notch activity (Peignon et al., 2011). This study showed that the Wnt/β-catenin signalling directly controls the activity of the *Hes1* promoter through the interaction with the Wnt/β-catenin effector, Tcf. Importantly, the two Tcf binding sites found for the human *Hes1* promoter are conserved in the mouse genome (Peignon et al., 2011), strongly suggesting that Wnt/β-catenin signalling may be regulating Hes1 expression also in mice.

Work from our laboratory found that MyT1, a paralog transcription factor to MyT1L, is able to counteract the activation by Notch of the *Hes1* proximal promoter region. Sequence analysis of the *Hes1* proximal promoter shows the existence of three MyT1 binding sites (AAGTT), which coincide with the *Hes1* promoter region with high enrichment for MyT1 (Figure 2B). I performed a comparative transcriptional assay between MyT1L and MyT1 that shows similar reduction of the activity of the *Hes1* proximal promoter, although with slightly higher efficiency for MyT1L. This is in line with previous studies, showing that MyT1L displays a higher affinity to the AAGTT motif comparatively to MyT1 (Besold et al., 2010; Gamsjaeger et al., 2008).

Ascl1-dependent reprogramming of MEFs to iN cells is controlled by Ascl1 due to its function as an "on-target" pioneer factor (Wapinski et al., 2013). This means that Ascl1 is able to target its *bona fide* target genes, independently of their chromatin accessibility in MEFs. Work in our laboratory also described that Hes1 acts as a transcriptional repressor of Ascl1 target genes in cultured NS/PCs. One interesting possibility is that Hes1 can repress the expression of Ascl1 target genes during neuronal reprogramming of MEFs. This repression may be the reason why iN cells have low levels of maturity observed in Ascl1 single-reprogramming (Chanda et al., 2014; Vierbuchen et al., 2010). MyT1L has been described to have a role at late stages of reprogramming by increasing the maturity of iN cells (Ambasudhan et al., 2011; Pang et al., 2011; Vierbuchen et al., 2010; Yoo et al., 2011). However, MyT1L ability to bind to its target genes in MEFs was still to be determined. I demonstrate through ChIP-qPCR that MyT1L binds to the *Hes1* proximal promoter in MEFs, two days after MyT1L induction. This suggests Hes1 as a possible target of MyT1L in reprogramming. Future experiments should demonstrate that MyT1L is able to downregulate the endogenous expression of Hes1 in MEFs. Moreover, I show in the same ChIP-qPCR experiment that Myt1L binds to a regulatory region of *Notch1*,

indicating *Notch1* as another target gene of MyT1L in MEFs. This suggests that MyT1L can bind to its available targets in MEFs at early stages of reprogramming.

During neurogenesis MyT1 competes with the RBPJ for their respective binding sites in the *Hes1* proximal promoter region to regulate Hes1 expression (Figure 2). In MEFs, I did not found evidence for Notch regulation of Hes1. Therefore, RBPJ does not activate the *Hes1* promoter by forming the RBPJ-NICD activator complex. This suggests that repression of Hes1 by MyT1L is not a result of the competition between MyT1L and the RBPJ-NICD activator complex, like MyT1 repression of Hes1 in NS/PCs (Figure 15A). Thus, MyT1L repression of Hes1 expression in MEFs would likely require direct repression activity at the *Hes1* promoter (Figure 15B). In support of this idea, MyT1 and MyT1L were shown to interact with Sin3B (Romm et al., 2005), a protein that mediates transcriptional repression by binding to histone deacetylases (HDACs) (Wolffe et al., 2000). Future experiments should demonstrate how MyT1L represses its target genes in MEFs reprogramming into iN cells (Figure 15B).

In reprogramming, MyT1L may indirectly promote the activation of Ascl1 target genes, and contributing to the maturation of neurons, by downregulating the expression of Hes1 (Figure 15C). In order to explore this hypothesis with Hes1 gain-of- and loss-of-function studies, I attempted at establishing a protocol to reprogram MEFs into neurons. However, this purpose was not achieved, mainly due to the high cell death rate 7 days post-induction. High cell death in neuronal reprogramming protocols is not exclusive to this study. Future experiments should therefore include some alterations to the protocol. Per example, high cell death was successfully overcome by the addition of the anti-apoptotic gene *BCL2L1* to reprogrammed neurons culture (Victor et al., 2014). Alternatively, co-culture with glia cells was also shown to extend the culture of Ascl1 single-reprogrammed iN cells by 2 weeks (Chanda et al., 2014). In addition, the rate of infection could be improved by adjusting the ratios of the various viruses. Finally, optimization of the lentivirus production to increase virus titter could be another solution towards an improved protocol.

MyT1L binds to the *Hes1* proximal promoter in MEFs 2 days after MyT1L induction, suggesting a role at early stages of reprogramming. This may lead to promoting iN cell maturation by counteracting Hes1 inhibition of Ascl1 target genes (Figure 15C). In addition, MyT1L was also shown to bind to the *Notch1* regulatory region in MEFs. Further studies should look at a genome-wide approach to identify other MyT1L targets that could be important for the reprogramming process. Finally, MyT1L downregulation of Hes1 in MEFs still needs to be assessed, as well as the importance of Hes1 regulation during reprogramming. Studies that look at the effects of gain-of- and loss-of-function of Hes1 during reprogramming and

identifying its targets in MEFs in a genome-wide level could shed a new light into the role of Hes1 in the reprogramming process.

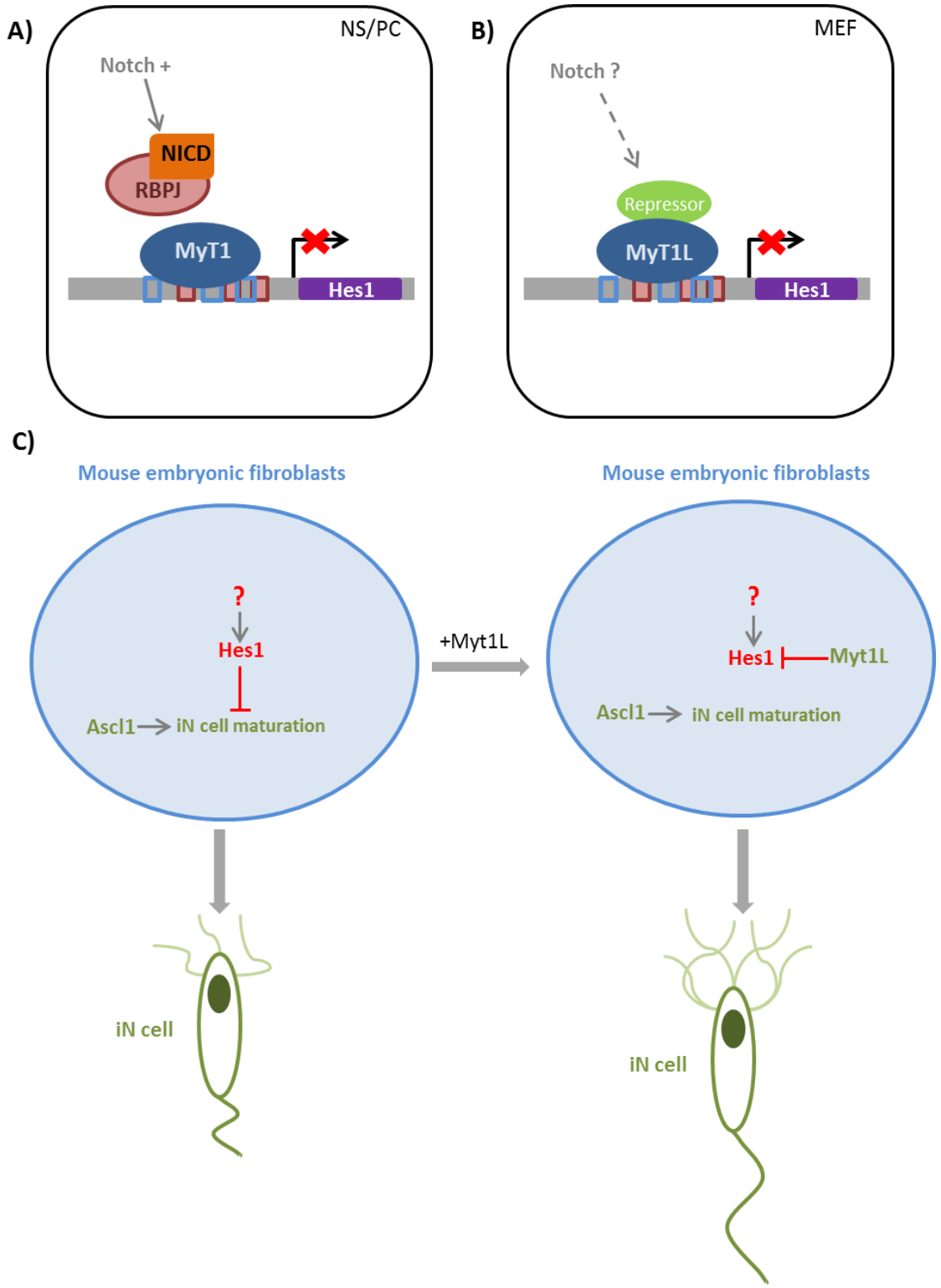

Figure 15 – Model of MyT1L repression of Hes1 in MEFs and MyT1L function in Ascl1-dependent reprogramming of MEFs into iN cells. (A) Scheme depicting the model of MyT1 repression of the Hes1 expression at the Hes1 proximal promoter. In neural stem/progenitor cells (NS/PCs) the MyT1 repression of Hes1 expression results from the competition between MyT1 and RBPJ for their respective

target sites in the Hes1 promoter. RBPJ is promoting Hes1 expression by interacting with the Notch intracellular domain (NICD) and forming the RBPJ-NICD activator complex. **(B)** In MEFs, I hypothesize that MyT1L repression of Hes1 occurs not by competing with the RBPJ-NICD activator complex but by direct repression activity at the Hes1 promoter through the recruitment of transcriptional repressors. **(C)** Ascl1 can reprogram MEFs into iN cells but with low levels of maturity (low morphological complexity and electrophysiological properties). Addition of MyT1L in combination with Ascl1 results in iN cells with higher levels of maturation. One possibility is that MyT1L indirectly promotes the expression of Ascl1 target genes responsible for neuronal maturation.

References

Ambasudhan, R., Talantova, M., Coleman, R., Yuan, X., Zhu, S., Lipton, S. a., Ding, S., 2011. Direct reprogramming of adult human fibroblasts to functional neurons under defined conditions. Cell Stem Cell 9, 113–118.

Andersson, E.R., Sandberg, R., Lendahl, U., 2011. Notch signaling: simplicity in design, versatility in function. Development 138, 3593–3612.

Basak, O., Taylor, V., 2007. Identification of self-replicating multipotent progenitors in the embryonic nervous system by high Notch activity and Hes5 expression. Eur. J. Neurosci. 25, 1006–1022.

Bellefroid, E.J., Bourguignon, C., Hollemann, T., Ma, Q., Anderson, D.J., Kintner, C., Pieler, T., 1996. X-MyT1, a Xenopus C2HC-type zinc finger protein with a regulatory function in neuronal differentiation. Cell 87, 1191–202.

Bertrand, N., Castro, D.S., Guillemot, F., 2002. Proneural genes and the specification of neural cell types. Nat. Rev. Neurosci. 3, 517–30.

Besold, A.N., Lee, S.J., Michel, S.L.J., Sue, N.L., Cymet, H.J., 2010. Functional characterization of iron-substituted neural zinc finger factor 1: Metal and DNA binding. J. Biol. Inorg. Chem. 15, 583–590.

Blanpain, C., Daley, G.Q., Hochedlinger, K., Passegué, E., Rossant, J., Yamanaka, S., 2012. Stem cells assessed. Nat. Rev. Mol. Cell Biol. 13, 471–476.

Borromeo, M.D., Meredith, D.M., Castro, D.S., Chang, J.C., Tung, K.-C., Guillemot, F., Johnson, J.E., 2014. A transcription factor network specifying inhibitory versus excitatory neurons in the dorsal spinal cord. Development 141, 3102–3102.

Casarosa, S., Fode, C., Guillemot, F., 1999. Mash1 regulates neurogenesis in the ventral telencephalon. Development 126, 525–534.

Castel, D., Mourikis, P., Bartels, S.J.J., Brinkman, A.B., Tajbakhsh, S., Stunnenberg, H.G., 2013. Dynamic binding of RBPJ is determined by Notch signaling status. Genes Dev. 27, 1059–1071.

Castro, D.S., Martynoga, B., Parras, C., Ramesh, V., Pacary, E., Johnston, C., Drechsel, D., Lebel-Potter, M., Garcia, L.G., Hunt, C., Dolle, D., Bithell, A., Ettwiller, L., Buckley, N., Guillemot, F., 2011. A novel function of the proneural factor Ascl1 in progenitor proliferation identified by genome-wide characterization of its targets. Genes Dev. 25, 930–45.

Castro, D.S., Skowronska-Krawczyk, D., Armant, O., Donaldson, I.J., Parras, C., Hunt, C., Critchley, J.A., Nguyen, L., Gossler, A., Gottgens, B., Matter, J.M., Guillemot, F., 2006. Proneural bHLH and Brn proteins coregulate a neurogenic program through cooperative binding to a conserved DNA motif. Dev. Cell 11, 831–844.

Chanda, S., Ang, C.E., Davila, J., Pak, C., Mall, M., Lee, Q.Y., Ahlenius, H., Jung, S.W., Südhof, T.C., Wernig, M., 2014. Generation of Induced Neuronal Cells by the Single Reprogramming Factor ASCL1. Stem Cell Reports 3, 282–296.

Conti, L., Pollard, S.M., Gorba, T., Reitano, E., Toselli, M., Biella, G., Sun, Y., Sanzone, S., Ying, Q.-L., Cattaneo, E., Smith, A., 2005. Niche-Independent Symmetrical Self-Renewal of a Mammalian Tissue Stem Cell. PLoS Biol. 3, e283.

Davis, R.L., Weintraub, H., Lassar, a B., 1987. Expression of a single transfected cDNA converts fibroblasts to myoblasts. Cell 51, 987–1000.

Gamsjaeger, R., Swanton, M.K., Kobus, F.J., Lehtomaki, E., Lowry, J. a, Kwan, A.H., Matthews, J.M., Mackay, J.P., 2008. Structural and biophysical analysis of the DNA binding properties of myelin transcription factor 1. J. Biol. Chem. 283, 5158–5167.

Geoffroy, C.G., Critchley, J. a, Castro, D.S., Ramelli, S., Barraclough, C., Descombes, P., Guillemot, F., Raineteau, O., 2009. Engineering of dominant active basic helix-loop-helix proteins that are resistant to negative regulation by postnatal central nervous system antineurogenic cues. Stem Cells 27, 847–56.

Giresi, P.G., Kim, J., Mcdaniell, R.M., Iyer, V.R., Lieb, J.D., 2007. FAIRE (Formaldehyde-Assisted Isolation of Regulatory Elements) isolates active regulatory elements from human chromatin. Genome Res. 877–885.

Hirata, H., Yoshiura, S., Ohtsuka, T., Bessho, Y., Harada, T., Yoshikawa, K., Kageyama, R., 2002. Oscillatory expression of the bHLH factor Hes1 regulated by a negative feedback loop. Science (80-.). 298, 840–843.

Hockemeyer, D., Soldner, F., Cook, E.G., Gao, Q., Mitalipova, M., Jaenisch, R., 2008. A drug-inducible system for direct reprogramming of human somatic cells to pluripotency. Cell Stem Cell 3, 346–53.

Hojo, M., Ohtsuka, T., Hashimoto, N., Gradwohl, G., Guillemot, F., Kageyama, R., 2000. Glial cell fate specification modulated by the bHLH gene Hes5 in mouse retina. Development 127, 2515–2522.

Huang, P., He, Z., Ji, S., Sun, H., Xiang, D., Liu, C., Hu, Y., Wang, X., Hui, L., 2011. Induction of functional hepatocyte-like cells from mouse fibroblasts by defined factors. Nature 475, 386–389.

Ieda, M., Fu, J.-D., Delgado-Olguin, P., Vedantham, V., Hayashi, Y., Bruneau, B.G., Srivastava, D., 2010. Direct Reprogramming of Fibroblasts into Functional Cardiomyocytes by Defined Factors. Cell 142, 375–386.

Imayoshi, I., Isomura, A., Harima, Y., Kawaguchi, K., Kori, H., Miyachi, H., Fujiwara, T., Ishidate, F., Kageyama, R., 2013. Oscillatory control of factors determining multipotency and fate in mouse neural progenitors. Science 342, 1203–8.

Ingram, W.J., McCue, K.I., Tran, T.H., Hallahan, A.R., Wainwright, B.J., 2008. Sonic Hedgehog regulates Hes1 through a novel mechanism that is independent of canonical Notch pathway signalling. Oncogene 27, 1489–500.

Ishikawa, Y., Onoyama, I., Nakayama, K.I., Nakayama, K., 2008. Notch-dependent cell cycle arrest and apoptosis in mouse embryonic fibroblasts lacking Fbxw7. Oncogene 27, 6164–74.

Iso, T., Kedes, L., Hamamori, Y., 2003. HES and HERP families: Multiple effectors of the notch signaling pathway. J. Cell. Physiol. 194, 237–255.

Kageyama, R., Ohtsuka, T., Hatakeyama, J., Ohsawa, R., 2005. Roles of bHLH genes in neural stem cell differentiation. Exp. Cell Res. 306, 343–348.

Kageyama, R., Ohtsuka, T., Shimojo, H., Imayoshi, I., 2008. Dynamic Notch signaling in neural progenitor cells and a revised view of lateral inhibition. Nat. Neurosci. 11, 1247–1251.

Kameyama, T., Matsushita, F., Kadokawa, Y., Marunouchi, T., 2011. Neuroscience Letters Myt / NZF family transcription factors regulate neuronal differentiation of P19 cells. Neurosci. Lett. 497, 74–79.

Kim, J.G., Armstrong, R.C., v Agoston, D., Robinsky, A., Wiese, C., Nagle, J., Hudson, L.D., 1997. Myelin transcription factor 1 (Myt1) of the oligodendrocyte lineage, along with a closely related CCHC zinc finger, is expressed in developing neurons in the mammalian central nervous system. J. Neurosci. Res. 50, 272–90.

Lanz, T. a., Hosley, J.D., Adams, W.J., Merchant, K.M., 2004. Studies of Aβ Pharmacodynamics in the Brain, Cerebrospinal Fluid, and Plasma in Young (Plaque-Free) Tg2576 Mice Using the γ-Secretase Inhibitor N2-[(2S)-2-(3,5-Difluorophenyl)-2-hydroxyethanoyl]-N1-[(7S)-5-methyl-6-oxo-6,7-dihydro-5H-dibenzo[b,d]azepin-7-. J. Pharmacol. Exp. Ther. 309, 49 –55.

Liu, Z.-J., Li, Y., Tan, Y., Xiao, M., Zhang, J., Radtke, F., Velazquez, O.C., 2012. Inhibition of fibroblast growth by Notch1 signaling is mediated by induction of Wnt11-dependent WISP-1. PLoS One 7, e38811.

Louvi, A., Artavanis-Tsakonas, S., 2006. Notch signalling in vertebrate neural development. Nat. Rev. Neurosci. 7, 93–102.

Lugert, S., Basak, O., Knuckles, P., Haussler, U., Fabel, K., Götz, M., Haas, C. a., Kempermann, G., Taylor, V., Giachino, C., 2010. Quiescent and active hippocampal neural stem cells with distinct morphologies respond selectively to physiological and pathological stimuli and aging. Cell Stem Cell 6, 445–456.

Marchetto, M.C., Gage, F.H., 2012. Modeling Brain Disease in a Dish: Really? Cell Stem Cell 10, 642–645.

Matsushita, F., Kameyama, T., Kadokawa, Y., Marunouchi, T., 2014. Spatiotemporal expression pattern of Myt/NZF family zinc finger transcription factors during mouse nervous system development. Dev. Dyn. 243, 588–600.

Matsushita, F., Kameyama, T., Marunouchi, T., 2002. NZF-2b is a novel predominant form of mouse NZF-2/MyT1, expressed in differentiated neurons especially at higher levels in newly generated ones. Mech. Dev. 118, 209–13.

Nishimura, M., Isaka, F., Ishibashi, M., Tomita, K., Tsuda, H., Nakanishi, S., Kageyama, R., 1998. Structure, chromosomal locus, and promoter of mouse Hes2 gene, a homologue of Drosophila hairy and Enhancer of split. Genomics 49, 69–75.

Ong, C.-T., Cheng, H.-T., Chang, L.-W., Ohtsuka, T., Kageyama, R., Stormo, G.D., Kopan, R., 2006. Target selectivity of vertebrate notch proteins. Collaboration between discrete domains and CSL-binding site architecture determines activation probability. J. Biol. Chem. 281, 5106–19.

Pang, Z.P., Yang, N., Vierbuchen, T., Ostermeier, A., Fuentes, D.R., Yang, T.Q., Citri, A., Sebastiano, V., Marro, S., Südhof, T.C., Wernig, M., 2011. Induction of human neuronal cells by defined transcription factors. Nature 476, 220–3.

Peignon, G., Durand, A., Cacheux, W., Ayrault, O., Terris, B., Laurent-Puig, P., Shroyer, N.F., Van Seuningen, I., Honjo, T., Perret, C., Romagnolo, B., 2011. Complex interplay between β-catenin signalling and Notch effectors in intestinal tumorigenesis. Gut 60, 166–176.

Pfisterer, U., Kirkeby, A., Torper, O., Wood, J., Nelander, J., Dufour, A., Björklund, A., Lindvall, O., Jakobsson, J., Parmar, M., 2011. Direct conversion of human fibroblasts to dopaminergic neurons. Proc. Natl. Acad. Sci. U. S. A. 108, 10343–10348.

Raposo, A.A.S.F., Vasconcelos, F.F., Drechsel, D., Marie, C., Johnston, C., Dolle, D., Bithell, A., Gillotin, S., van den Berg, D.L.C., Ettwiller, L., Flicek, P., Crawford, G.E., Parras, C.M., Berninger, B., Buckley, N.J., Guillemot, F., Castro, D.S., 2015. Ascl1 Coordinately Regulates Gene Expression and the Chromatin Landscape during Neurogenesis. Cell Rep. 10, 1544–1556.

Romm, E., Nielsen, J.A., Kim, J.G., Hudson, L.D., 2005. Myt1 family recruits histone deacetylase to regulate neural transcription. J. Neurochem. 93, 1444–53.

Shimojo, H., Ohtsuka, T., Kageyama, R., 2011. Dynamic expression of notch signaling genes in neural stem/progenitor cells. Front. Neurosci. 5, 78.

Takahashi, K., Yamanaka, S., 2006. Induction of pluripotent stem cells from mouse embryonic and adult fibroblast cultures by defined factors. Cell 126, 663–76.

Vasconcelos, F.F., Castro, D.S., 2014. Transcriptional control of vertebrate neurogenesis by the proneural factor Ascl1. Front. Cell. Neurosci. 8, 1–6.

Victor, M.B., Richner, M., Hermanstyne, T.O., Ransdell, J.L., Sobieski, C., Deng, P.-Y., Klyachko, V.A., Nerbonne, J.M., Yoo, A.S., 2014. Generation of Human Striatal Neurons by MicroRNA-Dependent Direct Conversion of Fibroblasts. Neuron 84, 311–323.

Vierbuchen, T., Ostermeier, A., Pang, Z.P., Kokubu, Y., Südhof, T.C., Wernig, M., 2010. Direct conversion of fibroblasts to functional neurons by defined factors. Nature 463, 1035–41.

Wang, S., Zhang, J., Zhao, A., Hipkens, S., Magnuson, M. a, Gu, G., 2007. Loss of Myt1 function partially compromises endocrine islet cell differentiation and pancreatic physiological function in the mouse. Mech. Dev. 124, 898–910.

Wapinski, O.L., Vierbuchen, T., Qu, K., Lee, Q.Y., Chanda, S., Fuentes, D.R., Giresi, P.G., Ng, Y.H., Marro, S., Neff, N.F., Drechsel, D., Martynoga, B., Castro, D.S., Webb, A.E., Südhof, T.C., Brunet, A., Guillemot, F., Chang, H.Y., Wernig, M., 2013. Hierarchical mechanisms for direct reprogramming of fibroblasts to neurons. Cell 155, 621–35.

Wilkinson, G., Dennis, D., Schuurmans, C., 2013. Proneural genes in neocortical development. Neuroscience 253, 256–73.

Wolffe, a P., Urnov, F.D., Guschin, D., 2000. Co-repressor complexes and remodelling chromatin for repression. Biochem. Soc. Trans. 28, 379–386.

Wu, Y., Liu, Y., Levine, E.M., Rao, M.S., 2003. Hes1 but not Hes5 regulates an astrocyte versus oligodendrocyte fate choice in glial restricted precursors. Dev. Dyn. 226, 675–689.

Yoo, A.S., Sun, A.X., Li, L., Shcheglovitov, A., Portmann, T., Li, Y., Lee-Messer, C., Dolmetsch, R.E., Tsien, R.W., Crabtree, G.R., 2011. MicroRNA-mediated conversion of human fibroblasts to neurons. Nature 476, 228–231.

Yoshiura, S., Ohtsuka, T., Takenaka, Y., Nagahara, H., Yoshikawa, K., Kageyama, R., 2007b. Ultradian oscillations of Stat, Smad, and Hes1 expression in response to serum. Proc. Natl. Acad. Sci. U. S. A. 104, 11292–11297.